

Probing i-motifs in a cellular model using a responsive nucleoside probe



A thesis submitted towards partial fulfilment of

BS-MS Dual Degree Programme

By

Samikshakiran Deepak Agham

(20141128)

Indian Institute of Science Education and Research, Pune

Under the guidance of

Thesis Supervisor

Dr. S. G. Srivatsan

Associate Professor

Department of Chemistry

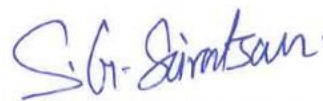
IISER-Pune

CERTIFICATE

This is to certify that this dissertation entitled "**Probing i-motifs in a cellular model using a responsive nucleoside probe**" towards the partial fulfilment of the BS-MS dual degree programme at the Indian Institute of Science Education and Research, Pune represents study/work carried out by "**Samikshakiran Deepak Agham**" at "Indian Institute of Science Education and Research, Pune" under the supervision of "**Dr.S.G.Srivatsan**, Associate Professor, Department of Chemistry" during the academic year 2018-2019.



Signature of Student



Signature of Supervisor

Declaration

I hereby declare that the matter embodied in the report entitled "**Probing i-motifs in a cellular model using a responsive nucleoside probe**" are the results of the work carried out by me at IISER Pune, under the supervision of **Dr.S.G.Srivatsan** and the same has not been submitted elsewhere for any other degree.



Signature of Student



Signature of Supervisor

Acknowledgement

I would like to express my sincere gratitude to my supervisor Dr. S. G. Srivatsan for guiding me throughout this project. I appreciate his attitude for constantly encouraging me in developing my research skills, presentation skills. I would also like to thank my TAC member Dr. H. N. Gopi who helped me in understanding and developing fundamentals of organic chemistry. I would also like to thank my lab members for helping and guiding me through the experiments. At the end I would like to acknowledge my friends and family for their constant support.

CONTENTS

Abstract.....	8
1.0 Introduction.....	9
2.0 Results and Discussion.....	11
2.1 Platform design.....	11
2.2 Studies inside AOT reverse micelles.....	22
3.0 Conclusion and Future perspective.....	28
4.0 Materials and methods.....	28
Supporting information/Appendix.....	37
References.....	46

List of Figures

S.N	Name of figure	Page No.
1	Structure of i-motif	9
2	Schematic representation of reverse micelles	11
3	Structure of the responsive nucleoside probe 5 and 7	12
4	Fluorescence study of nucleoside 7	13
5	HPLC chromatogram of modified ONs (10 and 8)	15
6	T_m analysis of modified (10 and 8) and control unmodified ONs(11 and 9)	15
7	Fluorescence plot of 10 and 8 modified ONs	17
8	CD profile of modified oligonucleotides	18
9	CD profile of modified (10 and 8) and control (11 and 9) unmodified ONs	19
10	Fluorescence plot of nucleoside 7 at different pH.	20
11	^{19}F and ^1H NMR of the modified ONs 10 and 8 at different pH.	22
12	DLS Study of RM of size W_o 20 at different pH	23
13	DLS study of RM of different W_o values.	23
14	Steady state fluorescence of 10 inside AOT Reverse Micelles.	24
15	CD profile of modified and unmodified ONs 10 and 11 inside RM	26
16	Fluorescence intensity of nucleoside 7 at different pH inside RM.	26
17	^{19}F NMR for nucleoside 7 at different concentration inside RM.	27
18	^{19}F NMR for nucleoside 7 at different pH inside RM.	28
19	Scheme 1	29
20	Scheme 2	30
21	Scheme 3	31

List of tables

S.N	Name of table	Page No.
1	Photophysical properties of nucleoside 5 in different microenvironments.	13
2	Fluorescence study of 7 as a function of increasing W_o values	14
3	pH values obtained for modified oligonucleotides 10 and 8	20
4	Diameter of reverse micelle at different pH	23
5	Diameter of reverse micelle at different W_o values	24

Abstract

G-rich sequences and C-rich sequences which can form G-quadruplexes and i-motifs have been considered as important regulatory elements in oncogenes. Although G-quadruplexes have been studied extensively inside cellular conditions but i-motif has been not explored. Given that C-rich sequences coexist along with G-quadruplexes development of a biophysical platform will be important. Here we have utilized a responsive nucleoside probe to investigate the structure of i-motif forming DNA oligonucleotides, H-telo (Human telomeric) and bcl2 (B-cell lymphoma), in aqueous buffer and inside a well-known cellular model, reverse micelles. The probe is composed of a microenvironment-sensitive fluorophore and ^{19}F NMR isotope label, which is synthesized by coupling fluorobenzofuran with 5-iodo-2'-deoxyuridine. The probe faithfully reports the changes in the microenvironment of the water core inside reverse micelles (RM). Probe incorporated into the loop region of different C-rich oligonucleotides H-telo and bcl2 does not hamper the formation of i-motif structure and its structural stability. Steady-state fluorescence and CD of modified oligonucleotides confirmed the formation of i-motif structure by these sequences at lower pH both in aqueous buffer and RM. Transition pH for the conversion of random coil to i-motif was determined by fluorescence and CD measurements. Further, ^{19}F and ^1H NMR of modified oligonucleotides reported formation of i-motif and transition from random coil to i-motif. Overall, the combination of responsive nucleoside probe and RM can be used to understand i-motif structures formed by individual C-rich sequences in near cellular environment.

1.0 Introduction

Nucleic acids play important biological roles like acting as genetic material, involving in gene regulation and catalysis. To perform these biological functions they adopt different secondary and tertiary structures.¹ Apart from its classical double helical structure, it can form other non-canonical structures which includes G-quadruplexes,² i-motifs³ etc. G-quadruplexes are formed by G-rich sequences and i-motifs are formed by C-rich sequences. Based on recent studies it was observed that these structures are mainly found clustered in regions which are important for biological functions such as regulatory regions of cancer causing genes and in telomeres (terminal regions of chromosomes).^{4,5} Although studies involving G-quadruplexes and its biological importance had been extensively studied^{6,7,8} but studies involving i-motif in cellular context is not well explored. Structure of i-motif consists of two parallel-stranded DNA duplexes. DNA duplexes are held together by intercalated cytosine–cytosine⁺ base pairs in an antiparallel orientation.⁹ (Figure 1). These i-motifs structures are mostly known to form at lower pH. However, in literature it is shown that formation of i-motif at physiological pH depends on various factors such as sequence itself and molecular crowding, ligand binding, negative superhelicity and certain modifications.^{10,11,12}

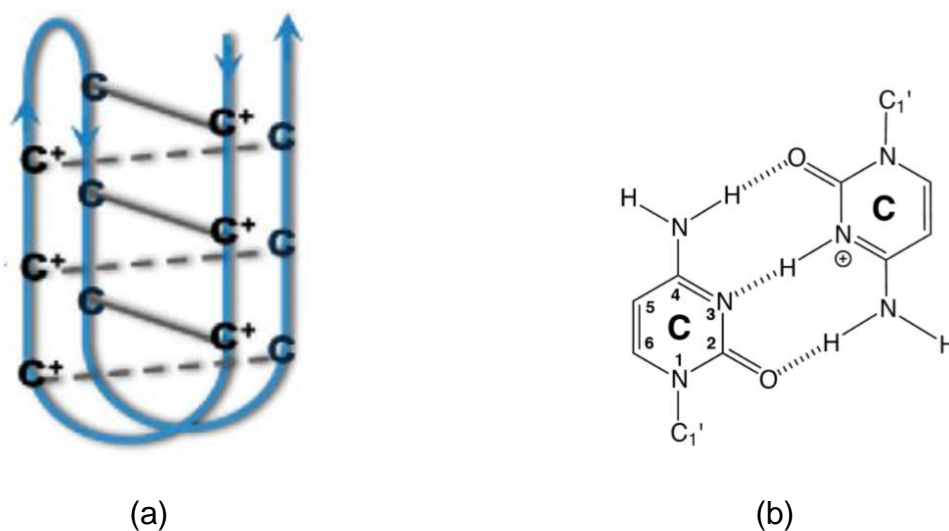


Figure 1: Schematic representation of i-motif structure. (a) i-motif structure, (b) hemi-protonated cytosine-cytosine base pairs.^{9,13}

Although existence of i-motif inside cell has remained debatable till date but recently this structure has been visualized in a structure specific manner using an

antibody fragment.^{14,15} Also recent evidences suggest that these structures are present in living cell and possibly are involved in biologically very important functions like replication and regulation of cancer causing gene expression.¹⁵ Therefore, this field in which i-motifs are being targeted, is emerging research area in medicinal chemistry.⁴ These structures are pH dependent and stable at lower pH. Due to this property it has several applications. Some groups have tried to use i-motif DNA as an attractive target for designing anticancer drug,⁴ development of 'I-switch' by Krishnan group was first example of i-motif based nanomachine. This machine not only is able to sense pH but it also reports pH changes along endosomal maturation inside both living cells in culture as well as in multicellular organism.¹⁶

Stability and folding topology of C-rich i-motif forming sequences depends on factors like number of cytosine residues, loop length and pH¹⁷. Various biophysical tools like NMR, X-Ray, and fluorescence have been used to study i-motif to random coil transition.^{6,7} Among these, fluorescence based tools provide efficient monitoring of formation of i-motif structure. A pair of pyrene-modified deoxyadenosines (an exciplex signalling system)¹⁸, "push-pull" fluorescent nucleoside analog, derived by fusing dimethylaniline to deoxycytidine are some of the fluorescent nucleoside analog probes,¹⁹ which have been used for monitoring pH dependent structural transition from i-motif to random coil. Although these studies were useful but they were mostly done in aqueous buffer so development of a biophysical platform to study i-motif inside cell like confinement will be highly useful. In this regard, we have used a fluorescence as well as ¹⁹F NMR responsive nucleoside probe. Using this probe, we successfully confirmed the formation of i-motif and transition from random coil to i-motif in aqueous buffer by performing studies such (T_m) UV-thermal melting, fluorescence, (CD) circular dichroism, ¹⁹F and ¹H NMR. This probe also successfully confirmed formation of i-motif and transition from random coil to i-motif inside RM.

2.0 Results and Discussion

2.1 Platform design: In order to probe i-motif formation in a cell-like confined environment we have developed an assay using a cellular model, AOT reverse micelle and responsive nucleoside probe. We have chosen reverse micelles as cellular model because it can solubilize most of the biomolecules and it is transparent to most of the spectroscopic techniques²⁰. AOT (Dioctyl sulphosuccinate

sodium) is used for the preparation of RM because it has the ability to solubilize substantial amount of water in various nonpolar solvents.^{21,22,23} Reverse micelles have four compartments as labelled in Figure 2: (1) intra micellar water pool; (2) aqueous interfacial region; (3) surfactant layer and (4) nonpolar phase.²⁴ Various properties like dynamics, polarity, viscosity, and proton-transfer efficiency of the water pool of reverse micelles are quite different from that of bulk water or aqueous buffer, in which most biophysical analyses are performed. Importantly, the size of the inside water pool of RM can be varied by changing W_o values. W_o is defined as ratio of concentration of water to concentration of AOT ($[water]/[AOT]$).⁷ Recently in our lab we have developed a micro-environment sensitive dual-app probe, fluorobenzofuran modified 2'-deoxyuridine. The probe has a responsive fluorophore and NMR compatible ^{19}F label. Both the ^{19}F and fluorescence properties of the probe are highly sensitive to small changes in the viscosity and polarity of the solvent.¹¹ The probe nicely distinguishes different G-quadruplex conformations of human telomeric DNA repeats and reported the preferred H-telo G-quadruplex conformation in live cell.¹³ Hence we have chosen this highly responsive probe to study i-motif structure formed by two biologically important H-telo and bcl2 oligonucleotides.⁹

Responsive nucleoside probe (**5**) and AOT RM were synthesized as reported. (Scheme 2). 5-Fluorobenzofuran was first stannylated, upon cross-coupling with 5-iodo-2'-deoxyuridine in the presence of a palladium catalyst gave 5-fluorobenzofuran-2'-deoxy corresponding phosphoramidite substrate was used by solid phase synthesis.⁷

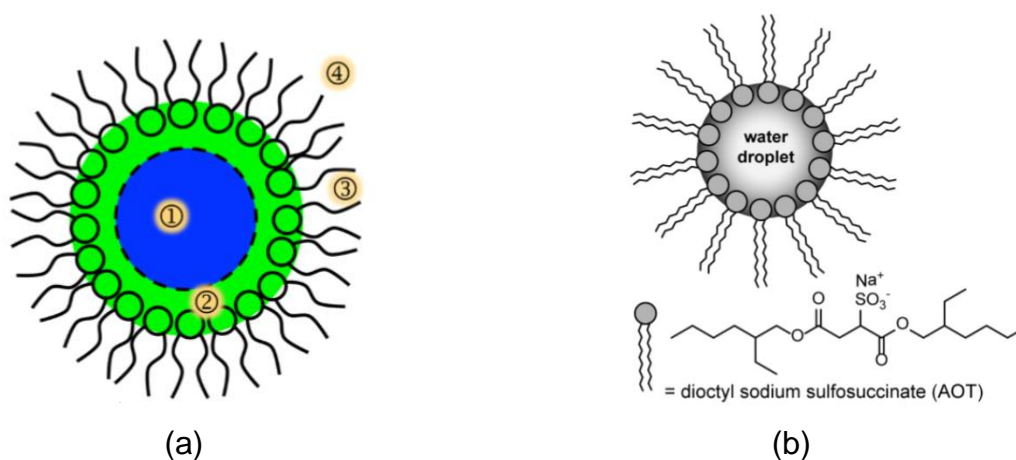


Figure 2: Schematic representation of reverse micelles: (a) Different domains of reverse micelles.²⁴ (b) AOT reverse micelle.²¹

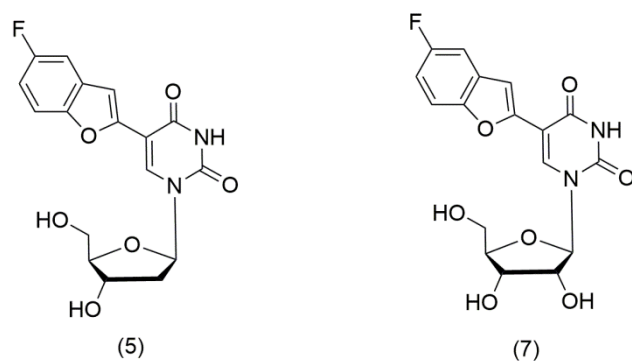


Figure 3: Structure of the responsive nucleoside probe **5** (deoxy version) and **7** (ribose version).

Nucleoside probe reported the microenvironment of the water pool of AOT RM:

The fluorescence and ^{19}F NMR properties of the nucleoside probe are highly sensitive to polarity and viscosity changes (Table 1)²⁵. With increase in polarity from dioxane ($\lambda_{\text{em}} = 400 \text{ nm}$) to water ($\lambda_{\text{em}} = 437 \text{ nm}$) there is increase in fluorescence intensity and red shift in emission maximum of nucleoside probe. Also with increase in viscosity from water to glycerol ($\lambda_{\text{em}} = 422 \text{ nm}$) there is increase in fluorescence intensity and blue shift in emission maximum. With increase in viscosity of medium in RM there is increase in quantum yield of nucleoside probe.²⁵ Before utilizing this probe to study i-motif formation inside RM, we examined whether the probe can sense the changes in the microenvironment of water core. Since the deoxy version of nucleoside **5** is less miscible in water and it tends to destabilize the RM, ribose version of nucleoside analog **7** was used.⁷ At first fluorescence study was done for AOT RM as a function of increasing W_o value. At low W_o ($W_o = 0.56$) value we get intense fluorescence peak at emission maximum 396 nm (Figure 4, Table 2). With increase in W_o there is decrease in fluorescence intensity with red shift in emission maximum. The fluorescence response of the probe largely depends on the location of the nucleoside probe inside RM.⁷ When W_o is low, there is no well-defined water pool. At this W_o probe is likely located at the interface region of AOT head group and water pool, which is more viscous and less polar as a result we observed high intense fluorescent peak with blue shift in emission maximum. Additionally, at low W_o , high value of anisotropy confirms the rigidification of the probe (Table 2). With increasing W_o , size of water pool inside RM increases and nucleoside probe permeates from interfacial region to aqueous micellar core region of RM which is less viscous and more polar (Figure 4). Nucleoside at this position is surrounded by

more polar and less viscous water medium and hence displays quenched fluorescence and red shift in emission maximum.⁷ Further lower anisotropy at higher W_o value proved the derigidification of the probe. Lifetime follows the same trend. It was observed that with increase in W_o there was decrease in average lifetime. From this observation we can conclude that the probe can successfully sense the micro-environment of the water pool of RM by displaying changes in fluorescence intensity and emission maximum.

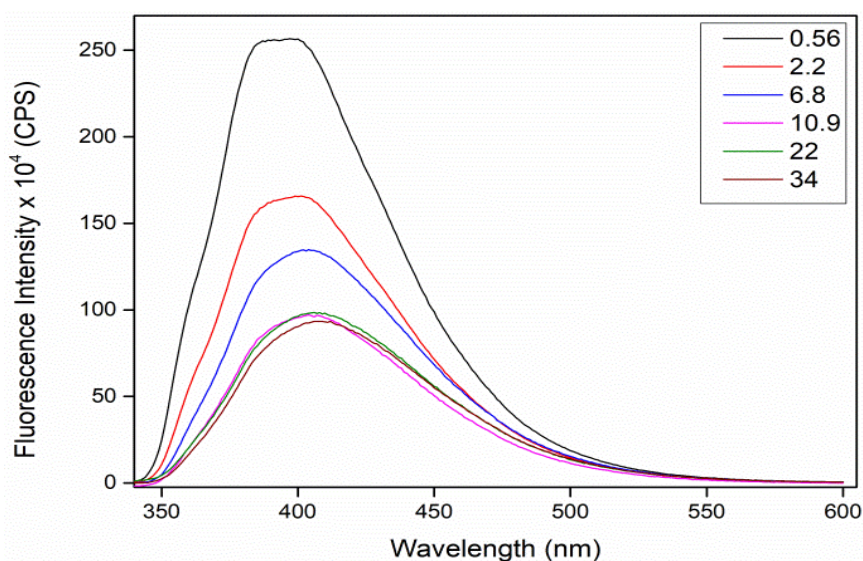


Figure 4: Fluorescence study of nucleoside **7** at different W_o values.

Table 1: Photophysical properties of nucleoside **5** in different microenvironments.²⁵

Solvent	λ_{em} (nm)	τ_{av} [a] (ns)	r [a]	Φ
Water	437	0.95	0.03	0.14
Methanol	420	0.81	nd	0.05
dioxane	400	0.85	nd	0.05
Ethylene glycol	423	0.99	0.18	0.22
glycerol	422	2.78	0.32	0.54

Standard deviation for quantum yield (Φ), average lifetime (τ_{av}) and anisotropy (r) in different solvents is ≤ 0.005 , ≤ 0.02 ns and ≤ 0.003 respectively. n.d. = not determined

Table 2: fluorescence study of **7** as a function of increasing W_o values.

W_o	λ_{em} (nm)	τ_{av} ^[a] (ns)	r ^[a]
0.56	396	2.27	0.193
2.2	393	2.23	0.211
6.8	397	2.12	0.197
10.9	403	1.98	0.164
22	405	1.96	0.157
34	406	1.96	0.148

[a] Standard deviation for average lifetime (τ_{av}) and anisotropy (r) at different W_o values are ≤ 0.09 and ≤ 0.01 , respectively.

Solid Phase Synthesis of i-motif forming sequences: Successfully the nucleoside was sensing the microenvironment of RM. So we decided to incorporate nucleoside into oligonucleotide by solid phase synthesis. i-motif forming modified H-telo **10** and bcl2 **8** oligonucleotides (ONs) were synthesized by following a reported procedure (Figure 5).¹³ Purposely, we have replaced thymine residue of loop region because replacing cytosine residues with probe **5** could hamper the efficiency of i-motif formation. The purity and integrity of ONs **10** and **8** were confirmed by HPLC and LCMS mass analysis (Figure 5).

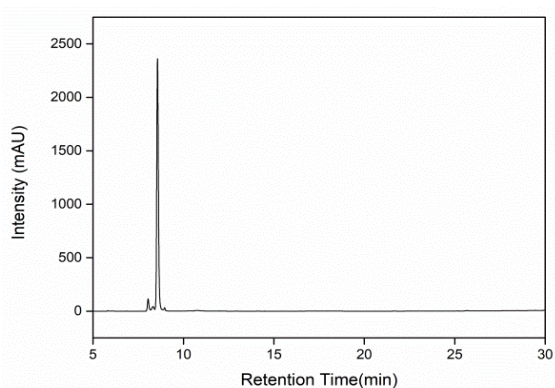
8 5' - d(CAG **CCC** CGC TCC CGC **CCC C5T** CCT **CCC** GCG **CCC** GCC CCT) -3'

9 5' - d(CAG **CCC** CGC TCC CGC **CCC** CTT CCT **CCC** GCG **CCC** GCC CCT) -3'

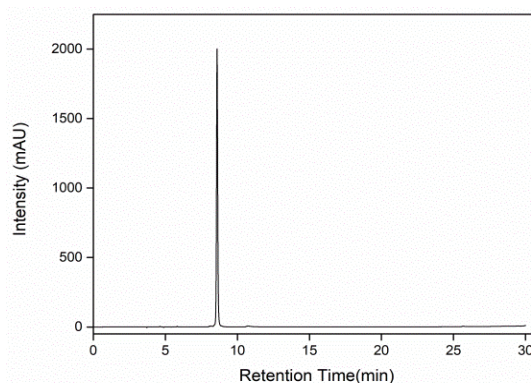
10 5' - d(**CCC** TAA **CCC 5AA** **CCC** TAA **CCC** TAA) -3'

11 5'- d(**CCC** TAA **CCC** TAA **CCC** TAA **CCC** TAA) -3'

(a)



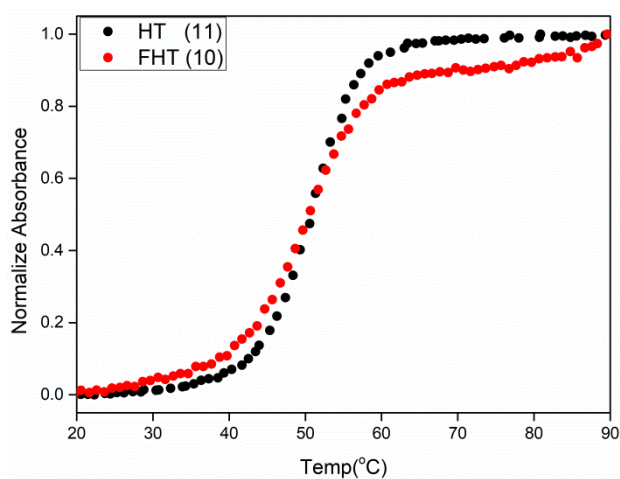
(b)



(c)

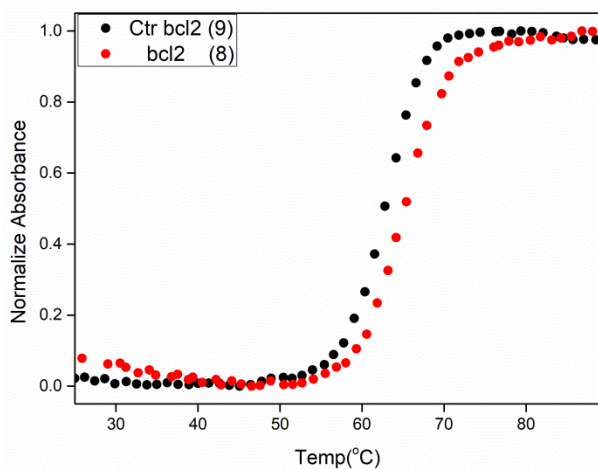
Figure 5: (a) **8** and **10** are modified i-motif forming ONs of bcl2 and H-Telo respectively. **9** and **11** are control unmodified ONs of bcl2 and H-Telo respectively. HPLC chromatogram of PAGE purified i-motifs forming sequences. (b) **8** (bcl2) and (c) **10** (H-telo)

UV-Thermal Melting (T_m) Analysis of Modified (10** and **8**) and control unmodified (**11** and **9**) ONs:** Before performing fluorescence study in aqueous buffer we wanted to examine whether the modified nucleoside **5** would hamper the stability of i-motif forms of bcl2 and H-Telo DNA ONs. For this we performed T_m analysis for both modified (**10** and **8**) and control unmodified (**11** and **9**) oligonucleotides. Similar T_m values for control and modified sequence revealed that modification did not hamper the stability of bcl2 and H-telo i-motif structures (Figure 6). The values were found to be close to the reported value.^{6,15}



(a)

	T_m Values
11 (Ctr H-telo)	52.3 ± 2.8
10 (H-telo)	50.5 ± 0.2



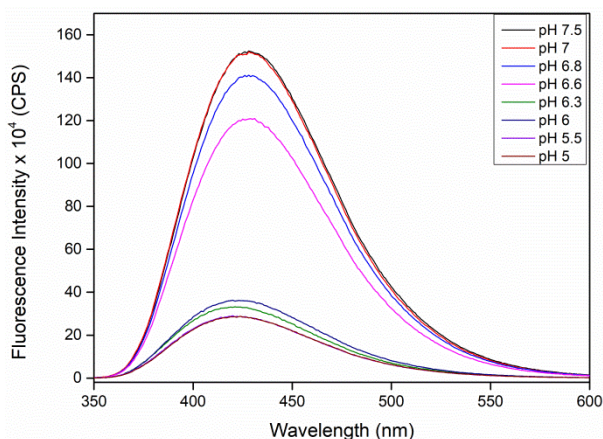
	T_m Values
9 (Ctr bcl2)	62.6 ± 1.3
8 (bcl2)	66.3 ± 1.2

(b)

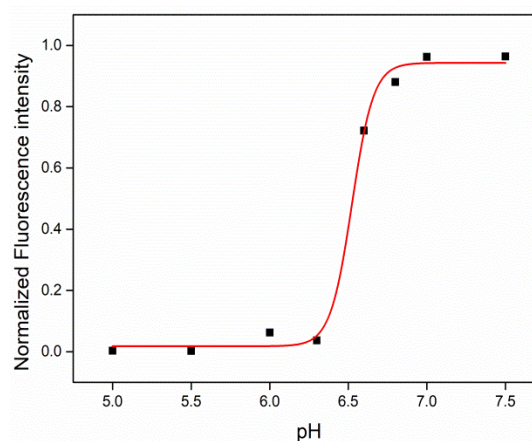
Figure 6: T_m analysis of modified (**10** and **8**) and control (**11** and **9**) DNA ONs. (a) T_m graph and table of **10** and **11**. (b) T_m graph and table of **8** and **9**.

Detection of i-motif Structure of Modified ONs (**10** and **8**) by Fluorescence:

The ability of the probe to report the formation of i-motif structures was evaluated by monitoring the changes in fluorescence intensity of H-telo (**10**) and bcl2 (**8**) ONs as a function of pH (7.5 – 5.0). At higher pH 7.5 a strong intense fluorescence peak whose emission maximum was centered around 428 nm was observed for both ONs **10** (Figure 7c) and **8** (Figure 7a). With decrease in pH from 7.4 to 5.0 there was a gradual pH dependent fluorescence quenching. However, there was no significant change in the emission maximum. Normalized fluorescence intensity at λ_{em} (428 nm) was plotted against pH. Plot was fitted using Boltzman equation, which provided the transition pH (ipH) for the conversion of random coil to i-motif (Table 3). The values were found to be close to the reported value.^{9,26,27}



(a)



(b)

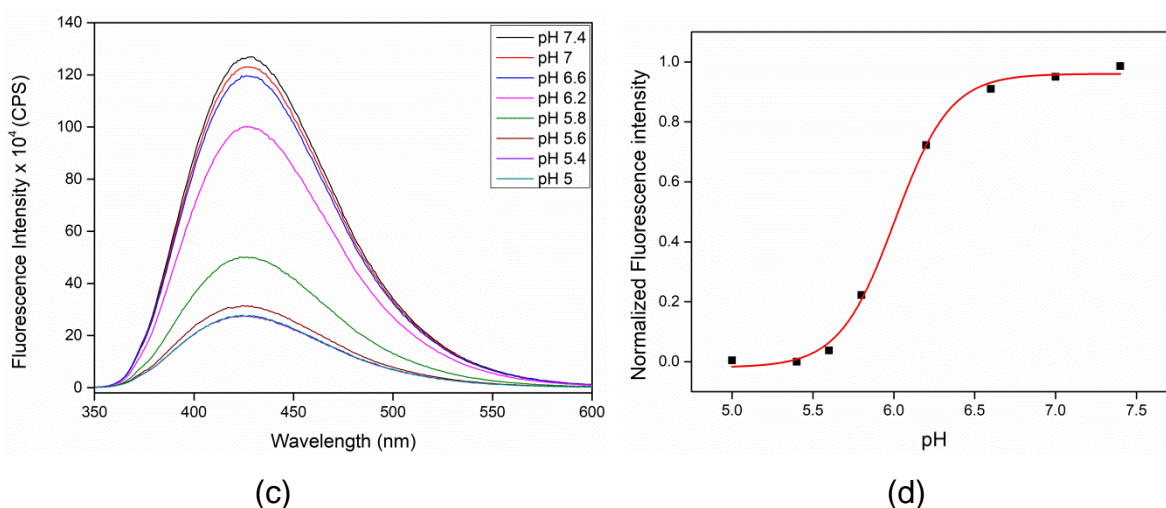
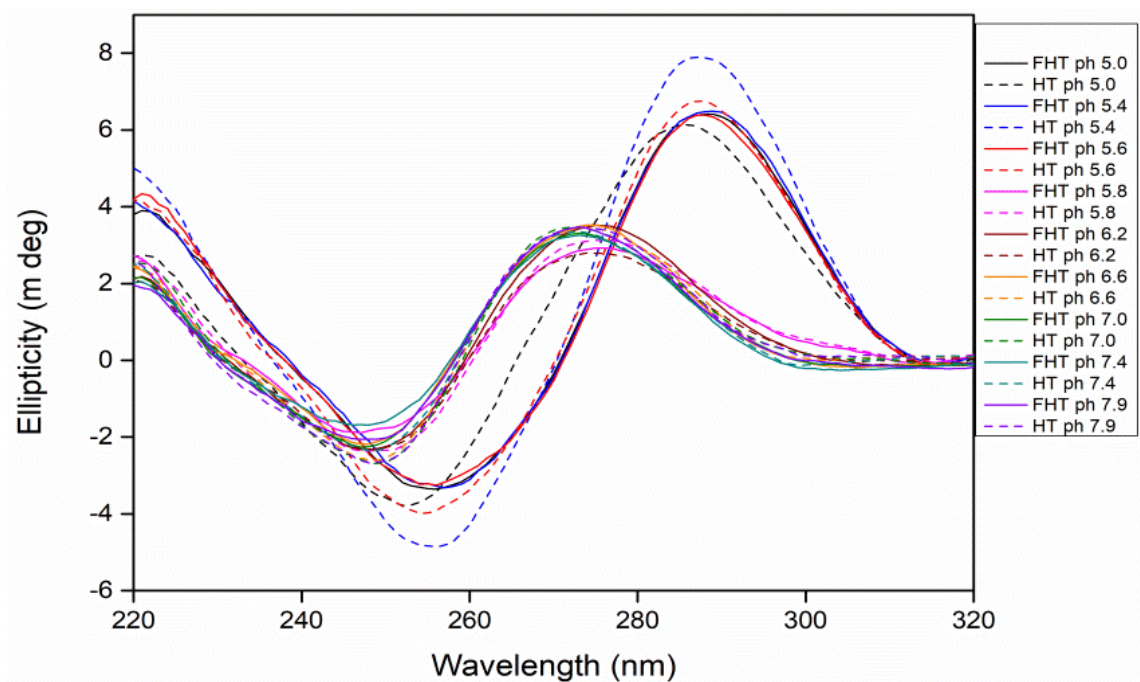
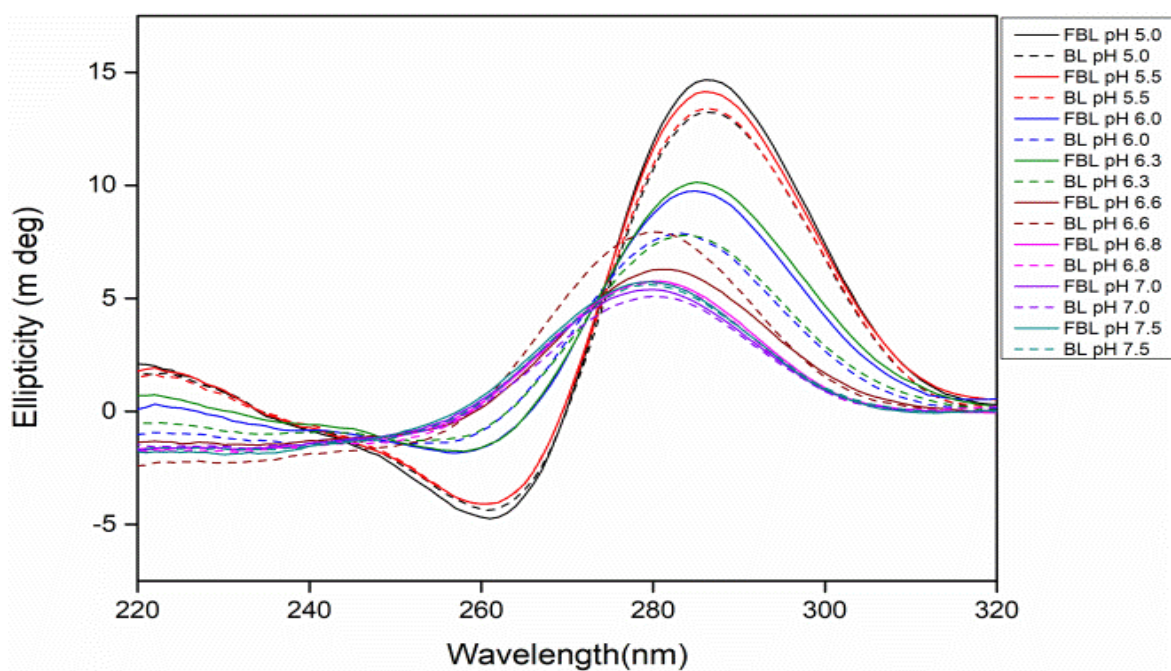


Figure 7: Fluorescence plot of **8** (bcl2) and **10** (H-telo) sequences: Graph (a) and (c) represents the change in fluorescence intensity of **8** and **10** at different pH respectively. Graph (b) and (d) represents Normalized fluorescence intensity graph which gives the ipH values 6.5 ± 0.03 and 6.0 ± 0.02 for modified sequences **8** and **10** respectively.

Circular dichroism analysis: To confirm the fact that changes in fluorescence intensity is due to the transformation of random coil to i-motif CD spectrum was recorded. A positive and negative peak at 275 nm and 248 nm shows the presence of a random coil at a higher pH (Figure 8a). As the pH was lowered, characteristic positive and negative peak at 287 nm and 257 nm for modified and control unmodified H-telo ONs **10** and **11** respectively, indicated the formation of i-motif structure. Similarly, CD profile of bcl2 ONs **8** and **9** gave characteristic positive and negative peak at 286 nm and 261 nm indicating the formation of i-motif at lower pH (Figure 8b). CD profile for modified (**10** and **8**) and control unmodified (**11** and **9**) ONs was similar. Further, ipH calculated from CD was almost similar to ipH calculated in fluorescence, which again indicates that the probe is minimally perturbing and faithfully reports the formation of i-motif structure (Figure 8 and 9).

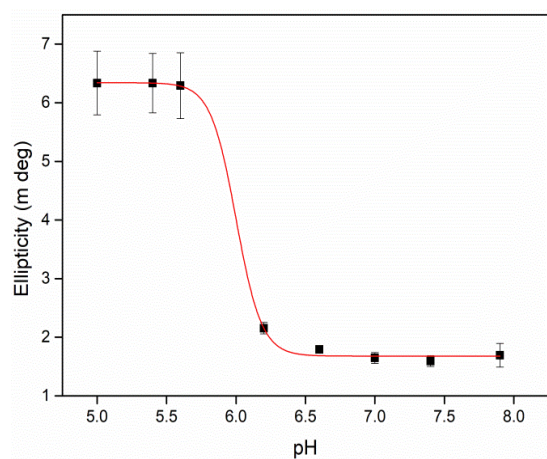


(a)

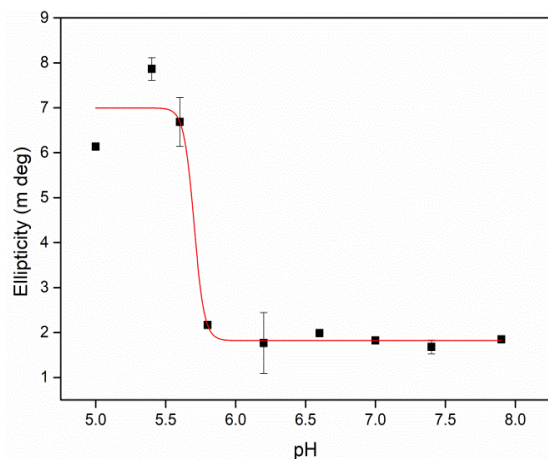


(b)

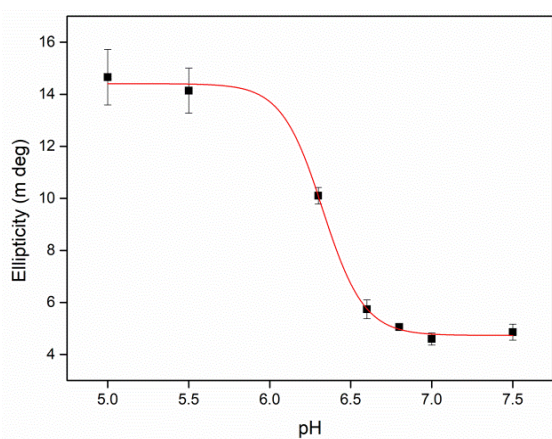
Figure 8 : CD profile of modified ONs **10** (H-telo) and **8** (bcl2). (a) CD profile for **10**. (b) CD profile for **8**.



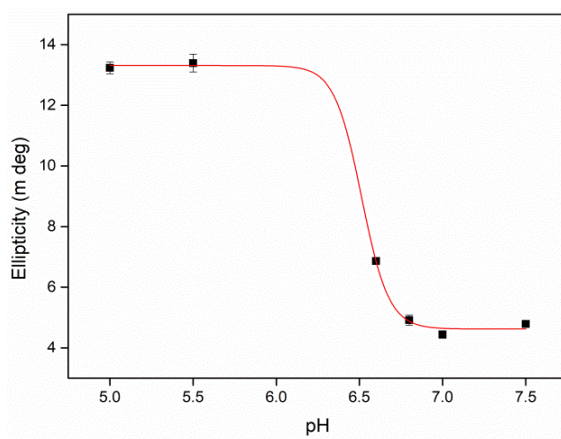
(a)



(b)



(c)



(d)

Figure 9: CD profile of modified **10** (H-telo) and **8** (bcl2) and control unmodified **11**(H-telo) and **9**(bcl2) ONs: (a) and (b) represents ellipticity of modified **10** and control unmodified **11** oligonucleotide. (c) and (d) represents ellipticity of modified **8** and control unmodified **9** oligonucleotides.

Table 3: ipH values obtained for modified oligonucleotides **10 (H-telo)** and **8(bcl2)**

ON	Name of technique	Average ipH
10	Steady state fluorescence; 6.0 ± 0.02 CD 5.7 ± 0.03	5.8 ± 0.02
8	Steady state fluorescence 6.5 ± 0.03 CD 6.3 ± 0.01	6.4 ± 0.02

Reported ipH for H-telo is 5.8 and for bcl2 it is 6.6.^{9,26,27}

In order to confirm that the changes in fluorescence intensity is only due to the structural changes in ONs, we recorded the fluorescence profile of free nucleoside **7** at different pH (7.5 – 5). It was observed that fluorescence was only slightly affected by changes in pH of the solution. This observation confirms that the fluorescence response is due to the structural changes in ONs, i.e., random coil to i-motif, and not due to the changes in nucleoside fluorescence at different pH.

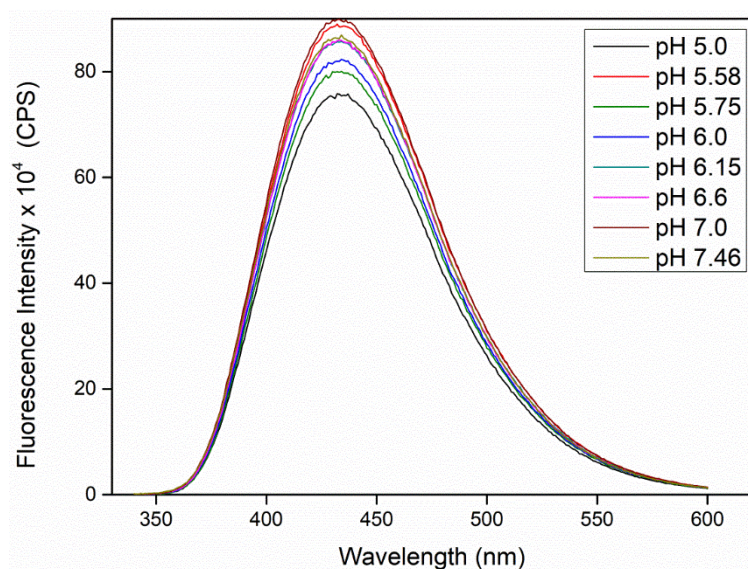
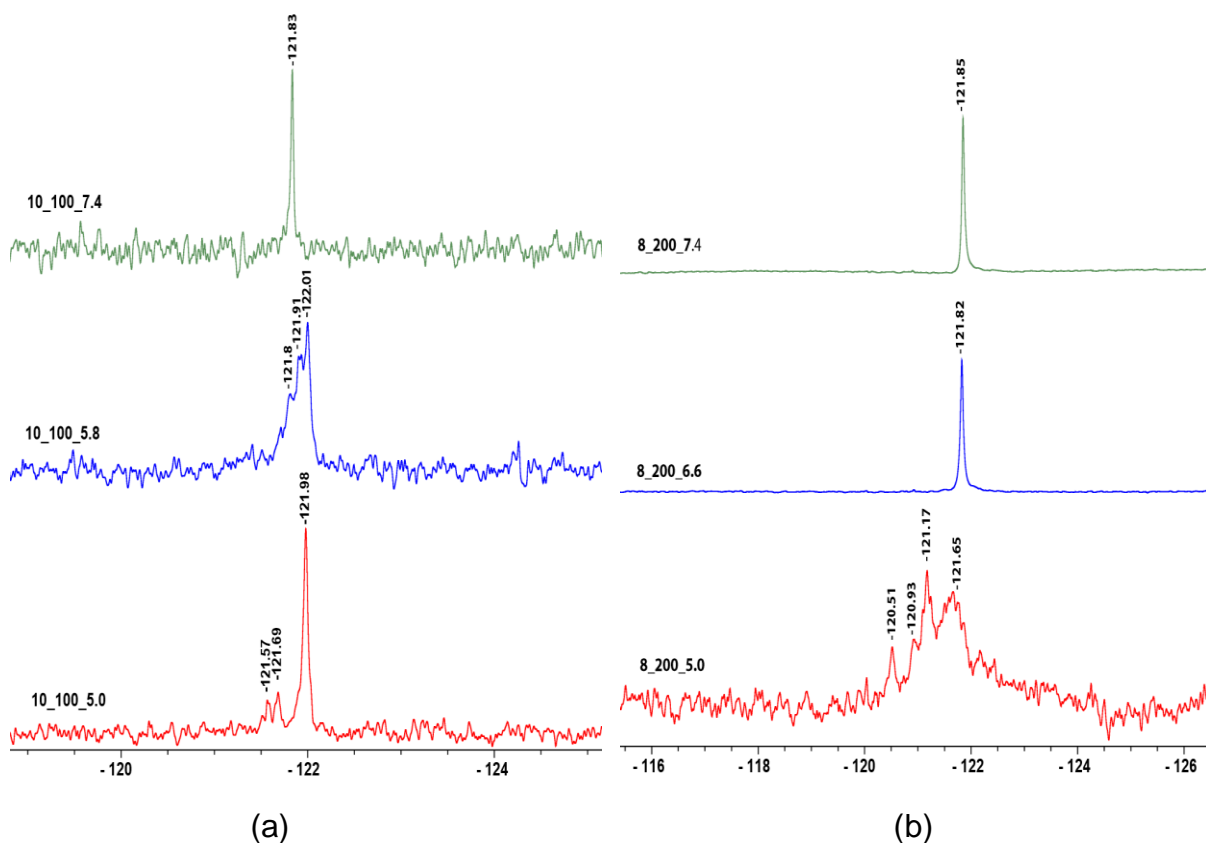


Figure 10: Fluorescence graph of nucleoside **7** at different pH.

^{19}F NMR label of also reports the formation of i-motif: Next, we studied the efficacy of ^{19}F label of the nucleoside probe to report the formation of i-motif structure of H-telo and bcl2 ONs. ON **10** (H-telo), at a lower pH 5.0, displayed a sharp signal at 121.98 ppm corresponding to i-motif form (Figure 11a). At a higher pH, presence of a sharp peak at -121.83 corresponding to a random coil was observed. Further, at near ipH value (pH= 5.8) a broad peak encompassing both i-motif and random coil was seen. The presence of i-motif was also confirmed by ^1H NMR experiments, where in the imino protons of i-motif typically comes around 15 ppm (Figure 11)^{26,28}. For bcl2 ON **8**, at lower pH 5.0 there is a mixture of peaks corresponding to the presence of multiple i-motif structures (Figure 11b). Similarly, in ^1H NMR at low pH 5.0 there were three peaks corresponding to i-motif formation. Hence, through ^{19}F and ^1H NMR presence of i-motif structures were detected.



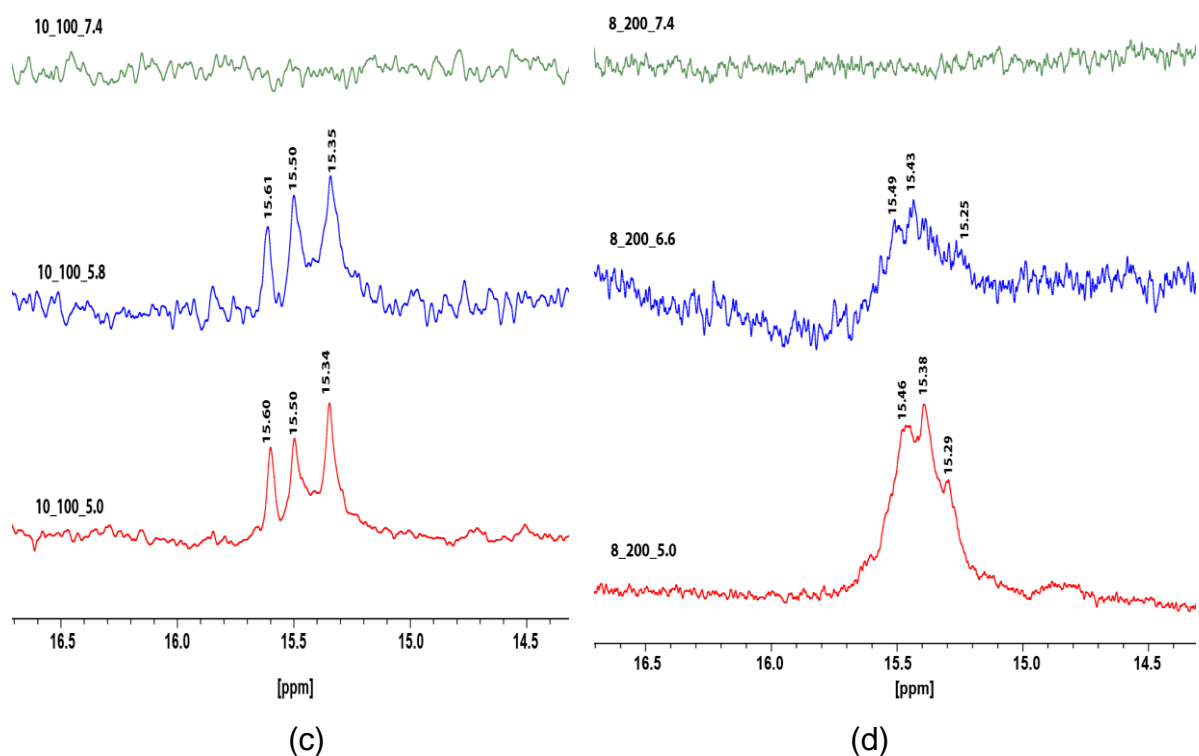


Figure 11: ^{19}F and ^1H NMR of the modified ONs **10** (H-telo) and **8** (bcl2) at different pH: (a) and (c) represents ^{19}F and ^1H NMR respectively for **10** at 5.0 (lower pH), 5.8 (ipH), and 7.4 (higher pH). (b) and (d) represents ^{19}F and ^1H NMR respectively for **8** at 5.0 (lower pH), 6.6 (ipH) and 7.4 (higher pH).

2.2 Studies in AOT Reverse Micelles

Through fluorescence, CD, ^{19}F and ^1H NMR studies in aqueous buffer, presence of i-motif, random coil and structural transformation of random coil into i-motif was confirmed. Our aim is to probe i-motifs in cell like confinement for which AOT RM was used. Hence it becomes important to carry out same set of studies in RM which were done in buffer conditions and check whether i-motifs are formed in similar fashion as in aqueous buffer conditions.

DLS study of RM: Before starting the studies in RM we need to know whether RM at different pH are forming and are they stable. Also the size of the RM which are being formed needs to be determined. To examine this, DLS analysis was done to determine the size of RM. This experiment was done as a set of two experiments with two different control. Firstly at different pH by keeping same W_o value and secondly at different W_o values. In first control by keeping same W_o value but

different pH, effect on size of RM was checked. It was observed that size of RM changes from 10 nm to 13 nm (Figure 12) and (Table 4). And with changing W_o there was change in the size of RM.(Figure 13)

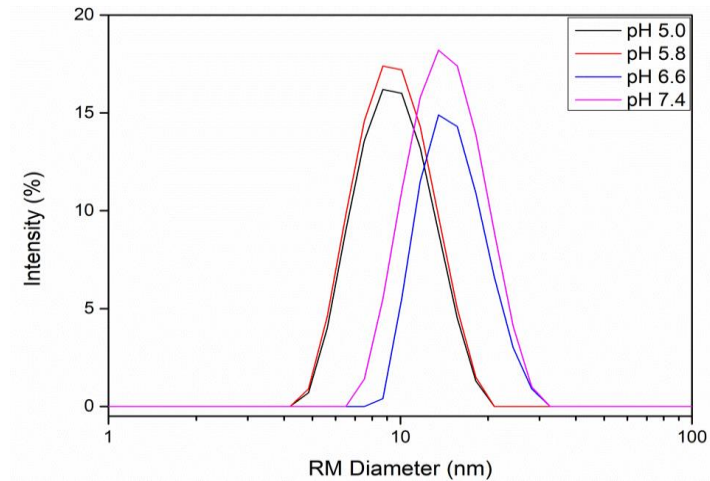


Figure 12: DLS Study of RM of size W_o 20 at different pH.

Table 4: Diameter of RM at different pH.

pH	Diameter (nm)
5.0	10.5 ± 0.8
5.8	10.2 ± 0.9
6.6	13.6 ± 0.9
7.4	13.5 ± 1.4

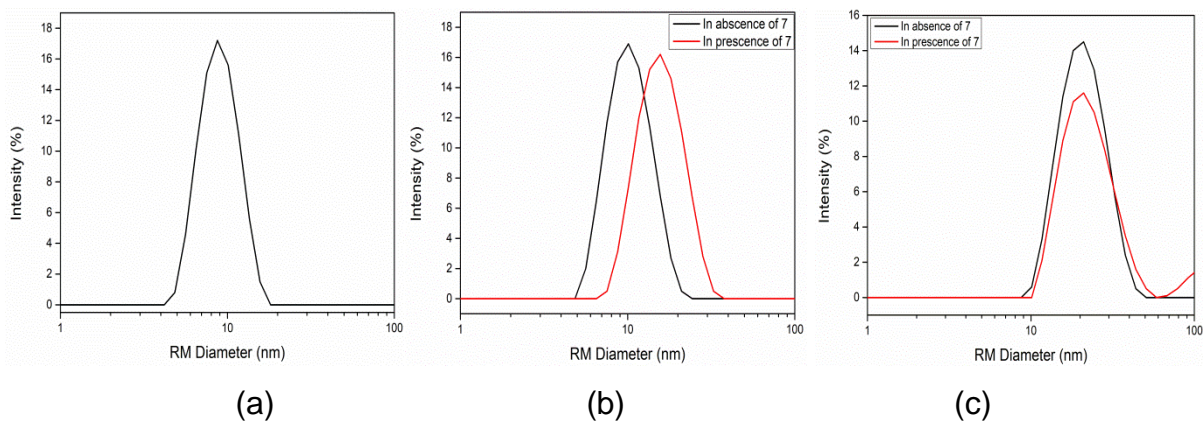


Figure 13: DLS study of RM at different W_o values.

Table 5: Diameter of RM at different W_o values.

W_o		Diameter (nm)	
		Without 7	With 7
6	(a)	8.2 ± 0.7	
20	(b)	10.6 ± 0.9	14.9 ± 1.3
34	(c)	21.3 ± 3.1	22.1 ± 1.9

Detection of i-motif formation of (H-telo) 10 ON in RM. Oligonucleotides at different pH was annealed and injected in the solution of RM. At higher pH 7.4 fluorescence intensity was high whose emission maximum was around 424 nm (Figure 14). With decrease in pH from 7.4 to 5.0 there was a gradual pH dependent fluorescence quenching. However, there was no significant change in the emission maximum with changes in pH. Results were similar to fluorescence study when was done inside aqueous buffer. Hence we concluded that probe **5** in RM successfully distinguishes i-motif and random coil based on changes in fluorescence intensity.

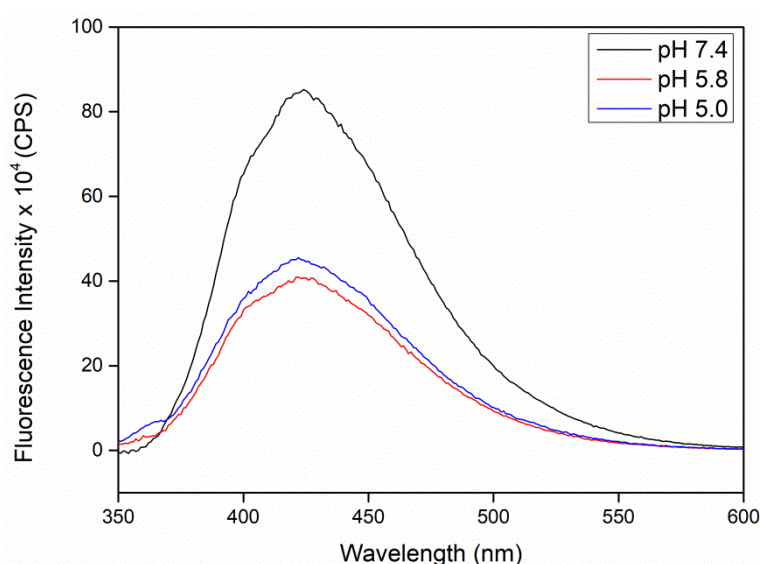


Figure 14: Steady state fluorescence of **10** inside AOT Reverse Micelles.

Circular Dichorism (CD) of modified ON 10 (H-telo) inside RM: To confirm that changes in fluorescence intensity is due to formation of i-motifs CD analysis was

performed for modified oligonucleotide **10** inside RM. Results were similar to when was done in aqueous buffer. At lower pH 5.0 distinct positive and negative peaks at 286 nm and 251 nm respectively confirmed the presence of i-motif. Whereas At higher pH 7.4 positive peak at 274 nm and negative peak at 248 nm corresponded to the presence of random coil.

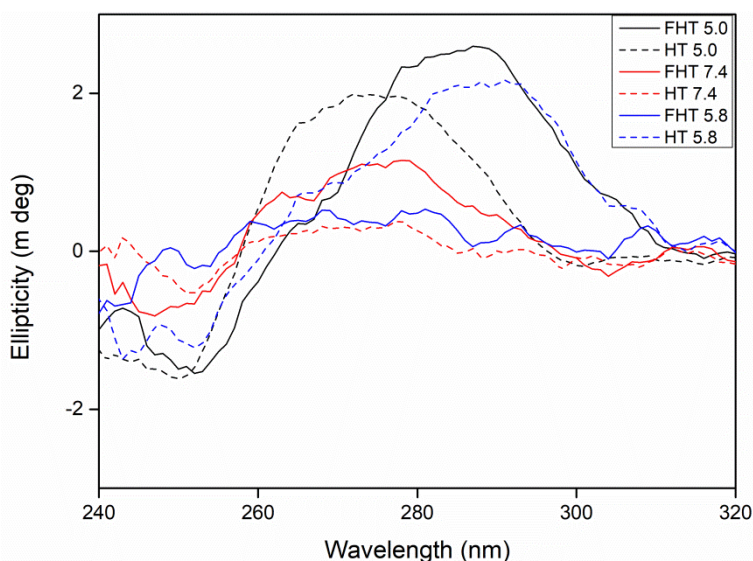


Figure 15: CD profile of modified and control unmodified oligonucleotides (H-telo) **10** and **11** inside RM: solid line represents modified sequence and dotted line represents unmodified sequence.

In order to confirm that changes in fluorescence intensity is only due to the structural changes in ONs, fluorescence profile of free nucleoside **7** at different pH (7.5 – 5) in RM was recorded. It was observed that inside RM the fluorescence intensity of **7** did not change with change in pH.(Figure 16) This confirms that the fluorescence response is due to the structural changes in ON and not due to the changes in nucleoside fluorescence at different pH inside RM.

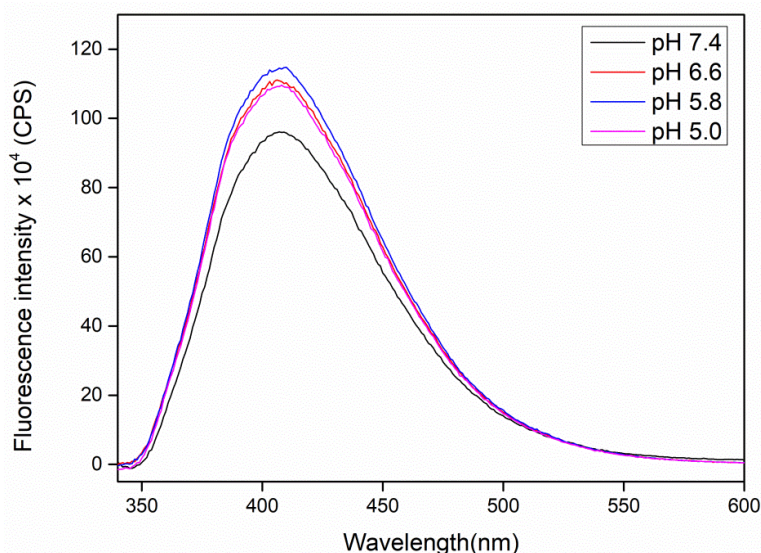


Figure 16: Fluorescence intensity of nucleoside **7** at different pH inside reverse micelles.

^{19}F NMR studies of free nucleoside **7 in different pH inside RM:** For doing NMR studies of ONs inside RM it is important that there is no shift in peak inside RM. Firstly concentration of nucleoside inside RM at which decent peak is obtained needed to be determined. Hence a control experiment was performed in which ^{19}F NMR was taken at same W_o ($W_o = 20$) but different concentration of nucleoside probe. Peak was obtained for all three concentration, 25 μM , 50 μM and 100 μM (Figure 17). Based on the results 50 μM concentration of nucleoside **7** was decided for further experiments.

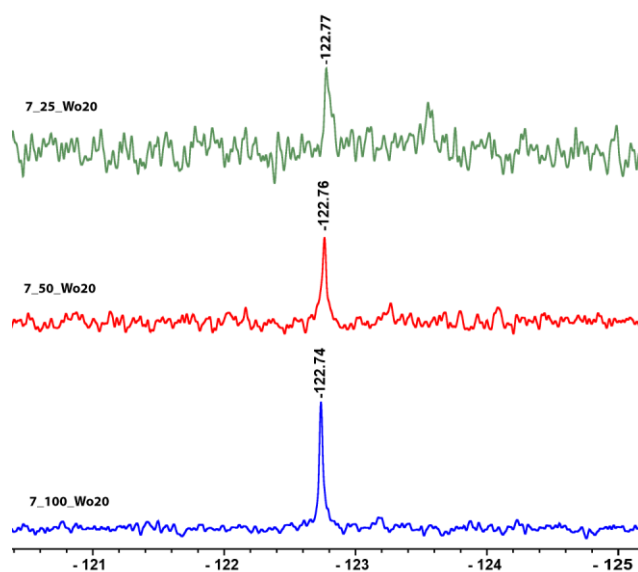


Figure 17: ^{19}F NMR for nucleoside **7** at different concentration inside RM.

After deciding on the concentration of the nucleoside next control experiment was to check whether position of peak changes at different pH. So at 50 μM concentration of nucleoside **7** ^{19}F NMR inside RM was taken at different pH (Figure 18). There was no change in the position of the peak, proving the fact that nucleoside is not sensitive towards pH changes in RM too.

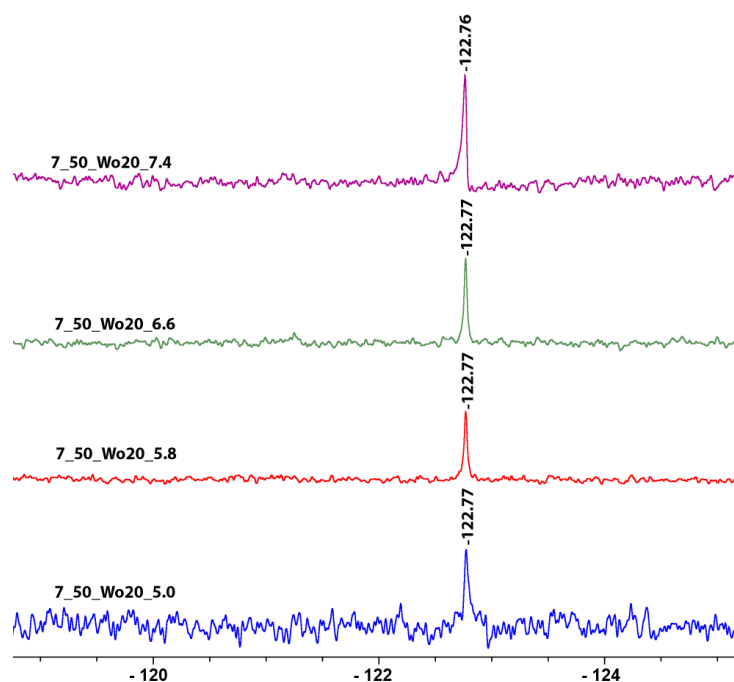
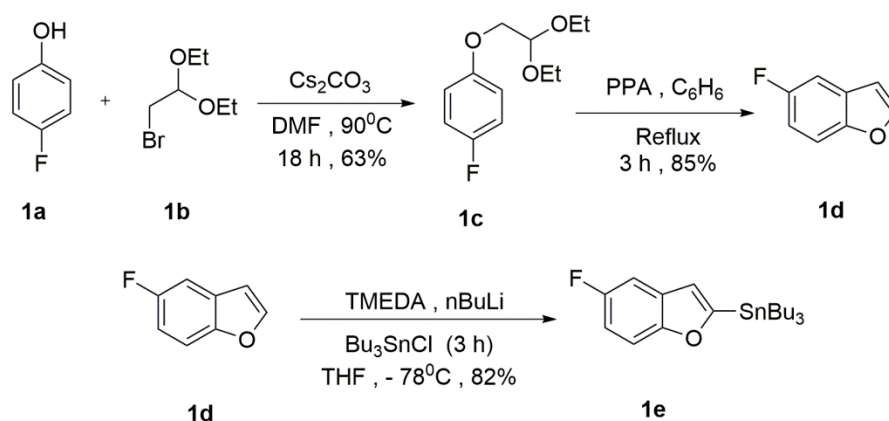


Figure 18: ^{19}F NMR for nucleoside **7** at different pH inside RM.

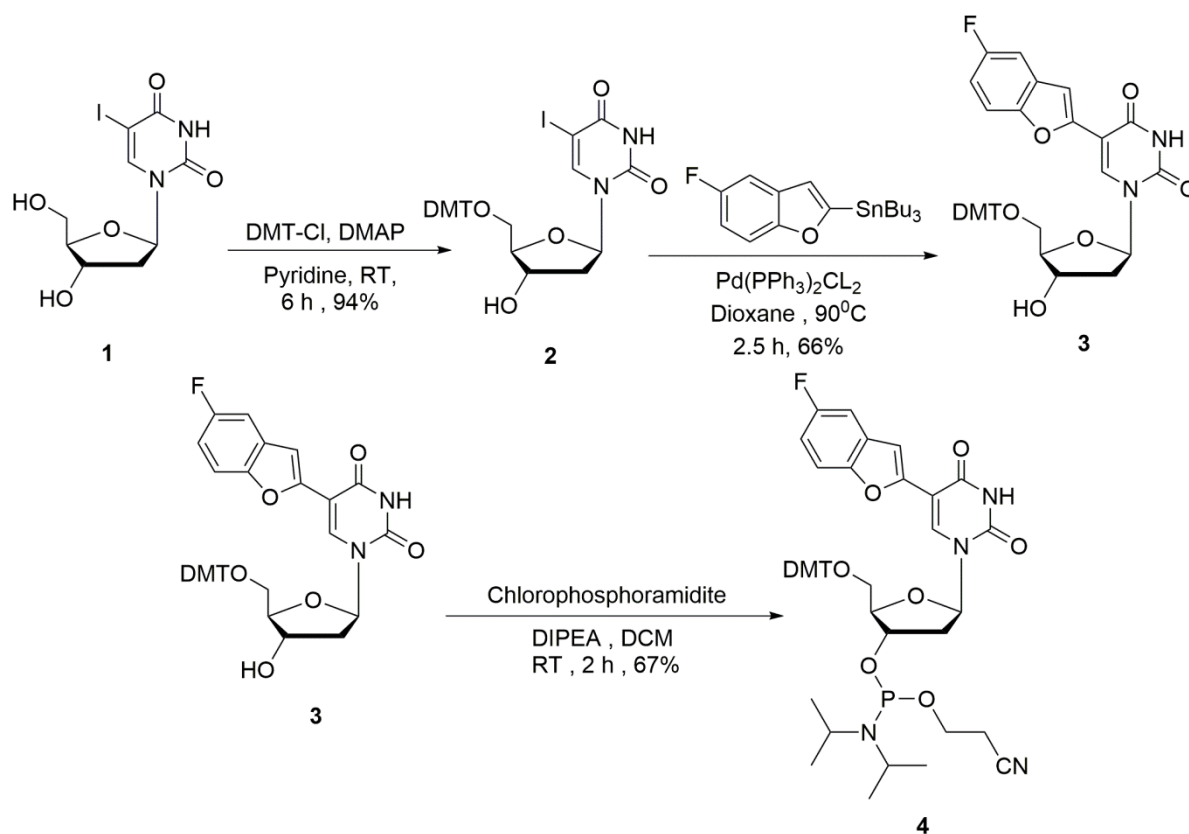
3.0 Conclusion and Future Perspective:

We came to know that probe **7** faithfully sense the microenvironment in RM. Incorporation of the probe **7** into H-telo and bcl2 DNA ONs does not hamper the stability of structural formation of i-motif. It also reports the structural transformation of random coil to i-motif via changes in fluorescence intensity and CD in both aqueous buffer and in RM. Structural transformation of random coil to i-motifs was further recognised by ^{19}F and ^1H NMR studies. These favourable properties of nucleoside probe suggest that it can be used further to study in detail the structure and dynamics of ONs in a cell like confined environment. Detection of i-motif and structural transformation of random coil to i-motif by CD, fluorescence and ^{19}F NMR for modified bcl2 in RM are currently under progress.

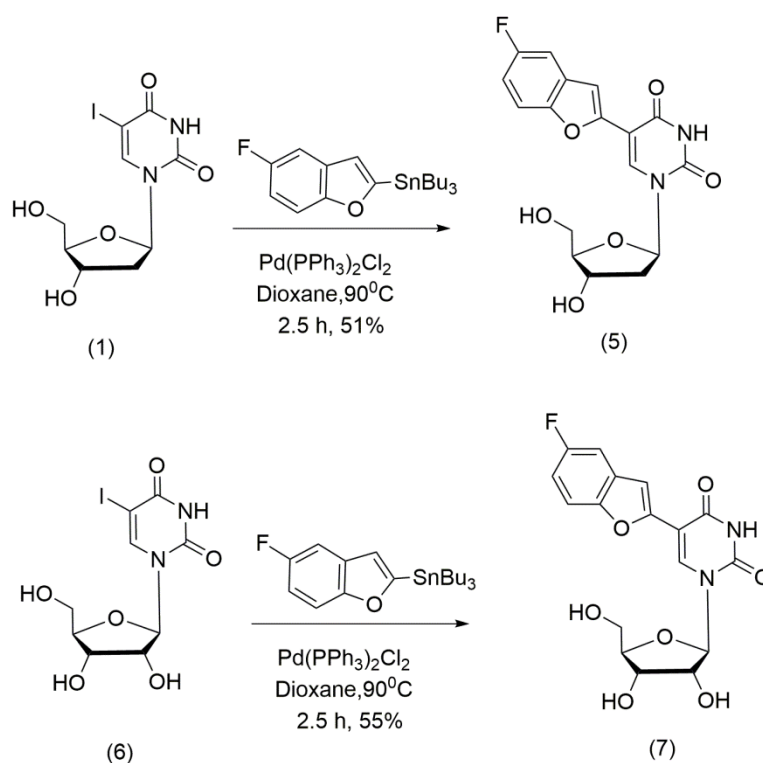
4.0 Materials and methods



Scheme 1: Synthesis of fluorophenol ether **1(c)**, 5-fluorobenzofuran **1(d)** stannylated Fluorobenzofuran **1(e)**.; Cs₂CO₃: Cesium Carbonate, DMF: Dimethyl Formamide, PPA: Polyphosphoric acid, TMEDA: Tetramethylenediamine.



Scheme 2: Synthesis of 5-fluorobenzofuran-2'-deoxyuridine (**3**) and corresponding phosphoramidite (**4**). DMAP: 4-Dimethylaminopyridine, DMT.Cl: 4,4'-Dimethoxytrityl chloride, Pd(PPh₃)₂Cl₂ : Bis(triphenylphosphine)palladium(II)dichloride, DCM: Dichloromethane, DIPEA: N,N-Diisopropylethylamine.



Scheme 3: Synthesis of 5-Fluorobenzofuran-modified-2'-deoxyuridine (**5**), Synthesis of 5-fluorobenzofuran-modified-2'-uridine (**6**) from modified nucleoside (**1**).

Synthesis of 4-Fluorophenoether 1(c): 2g (17.8 mmole, 1 equiv) of 4-Fluorophenol to it 40mL of DMF (Dimethylformamide) was added, then reaction was kept for stirring. Then 8.72g (26.79 mmole, 1.5 equiv) of Cs₂CO₃ (Cesium Carbonate) was added. Then 3.21mL (21.36 mmole, 1.2equiv) of Bromoacetaldehyde diethyl acetal was added to the reaction mix. Addition was carried out in N₂ medium. Then reaction was kept for heating for about 18 hrs. TLC medium: 30% EtOAc (Ethyl Acetate) in Hexane. 120mL of water, 100mL of EtOAc was added to (approx.) 40 mL of reaction

mix. Again 100mL of EtOAc was added. Subsequently washing was given with the EtOAc two times. Finally washing was given with 100mL of water and then Brine solution (Sat. NaCl) to EtOAc layer. Finally Na₂SO₄ (sodium sulphate) was added. Column was done in Ethyl acetate and Hexane. Obtained yield is 8.9 g. Hence yield percentage is 63%. ¹H NMR (400MHz, CDCl₃) δ = 6.97-6.92 (m, 2H), 6.86 – 6.83 (m, 2H), 4.81-4.79 (t, *J* = 5.2 Hz, 1H), 3.96 (d, *J* = 5.2 Hz, 2H), 3.75-3.73 (m, 2H), 3.64-3.61 (m, 2H), 1.25-1.21 (t, *J* = 7.1Hz, 6H); ¹³C NMR (400 MHz, CDCl₃): δ (ppm) 116.0, 115.8, 115.7,115.7, 100.5, 77.4,77.2, 77.1, 76.7, 69.2, 62.2, 51.0, 15.4.

Synthesis of 5-fluorobenzofuran 1(d): 2.6 g (9.13 mmole, 1 equiv) of Fluorophenol Ether, 3.7 g (10.96 mmole, 1.2 equiv) of PPA (Polyphosphoric acid) was taken in an RB and reaction mix was kept for vacuum dry for 15-20 min. Then finally 70 mL of Benzene was added in N₂ condition. Reaction was kept for heating (reflux) for about 3 hrs. TLC medium: 100% Hexane. After removing the reflux setup RB was kept to cool down. PPA was allowed to settle down and the reaction mix was decanted into another RB. Washing was given by DCM to the RB. Column was loaded in the 100% Hexane. Obtained yield is 3.6 g. Yield percentage is 85%. ¹H NMR (CDCl₃, 400MHz); δ = 7.64 (d, *J* = 2.2 Hz, 1H), 7.43-7.40 (m, 1H), 7.26-7.23 (dd, 1H), 7.03-6.98 (m, 1H), 6.73(d, *J* = 1H); ¹³C NMR (400 MHz, CDCl₃): δ (ppm) 160.5, 158.1, 151.3, 146.7, 112.2, 112.1, 112.0, 119.5, 106.9, 106.9,106.5.

Synthesis of stannylated fluorobenzofuran 1(e): 3.6 g (26.45 mmole, 1 equiv) of fluorobenzofuran and to it 72 mL of THF (Tetrahydrofuran) was added. Then at room temperature 4.67 mL (31.74 mmole, 1.2 equiv) TMEDA (Tetramethylenediamine) was added. Then bowl in which RB was kept was filled with Dry ice. Then Acetone is poured on the dry ice covering RB for more cooling. After some time with plastic syringe nBuLi (nButyl Lithium) was added dropwise. After 1.5 hrs 8.6 mL (31.74 mmole, 1.2 equiv) of Bu₃SnCl (Stannyl Chloride) was added. In total the reaction was kept for 3 hrs. TLC medium 100% Hexane. Solution of EtOAc in Hexane in 1:1 proportion (total 300mL) was made. RB was allowed to cool down then saturated solution of NH₄Cl was added dropwise. Reaction mix turns turbid yellow and addition was continued till no more solid was formed and finally it was transferred to the separating funnel. It was given washing with the EtOAc in Hexane solution two times (150mL each time). Finally washing was given by Brine solution and organic and aqueous layer were collected separately. Finally Na₂SO₄ was added to organic layer.

Column was loaded in 100% Hexane. Obtained yield is 9.02 g. Yield percentage is 82%. ¹H NMR (CDCl₃, 400MHz); δ = 7.40-7.37 (m, 1H), 7.18-7.16 (m, 1H), 6.95-6.89 (td, 1H), 6.84 (d, 1H), 1.60-1.55 (m, 6H), 1.26-1.25 (dd, 6H), 1.15-1.12 (m, 6H), 0.89-0.87 (m, 9H). ¹³C NMR (400 MHz, CDCl₃): δ (ppm) 118.2, 118.2, 111.5, 111.4, 111.1, 110.8, 105.7, 105.5, 32, 29.2, 27.2, 22.6, 14.4, 13.6, 10.8.

DMT protected 5-iodo-2'-deoxyuridine (2): 500 mg (1.41 mmol, 1 equiv.) of 2-deoxy-5-iodo uridine, 717 mg (2.12 mmol, 1.5 equiv) of DMT-Cl and 86 mg (0.71 mmol, 0.5 equiv) DMAP was added and kept for high vacuum for 1 hour. Finally 15 mL of pyridine under nitrogen atmosphere was added. Reaction was kept for stirring for 6 h. TLC in 5% methanol in DCM, 0.5% TEA (Triethyl amine). Column was done in methanol, DCM system. Obtained yield is 0.87 g, yield percentage is 94%.; ¹H NMR (CDCl₃, 400 MHz);δ (ppm) = 8.13 (s, 1H), 7.42-7.40 (d, 2H), 6.86 (s, 2H), 6.84 (s, 2H), 6.31- 6.28 (dd, 1H), 4.56-4.53 (td, 1H), 4.08-4.06 (q, 1H), 3.80 (s, 6H), 3.45-3.41 (dd, 1H), 3.39-3.35 (dd, 1H), 2.49-2.44 (m, 1H), 2.33-2.26 (m, 1H), 1.88-1.87 (d, 1H). ¹³C NMR (400 MHz, CDCl₃): δ (ppm) 158.8, 144.6, 144.5, 135.7, 135.5, 130.2, 128.2, 127.1, 113.5, 87.1, 86.7, 85.8, 64.0, 55.5, 53.1, 30.0.

5-Fluorobenzofuran-modified 5'-O-DMT-2'-deoxyuridine (3): 578 mg (0.88 mmole, 1 equiv) of tritylated 2-deoxy-5-iodouridine, 0.561 g (1.32 mmole, 1.5 equiv) of stannylated FBF (fluorobenzofuran) and finally 16 mL of dioxane was added in N₂ conditions. Reaction mixture was degassed for about 40 min. Catalyst Pd(PPh₃)₂Cl₂ Bis(triphenylphosphine) palladium (II) chloride was added and reaction mix was kept for heating in the oil bath at around 110°C. Reaction was kept for 3.5 hrs (approx.). TLC medium: 5% methanol, 1% TEA in DCM. Column was done in methanol, DCM system. Obtained yield is 0.39 g. Yield percentage is 66%.; ¹H NMR (CDCl₃, 400 MHz);δ (ppm) = 8.51 (s, 1H), 7.51-7.48 (m, 2H), 7.38-7.35 (m, 5H), 7.22-7.18 (dd, 2H), 7.12-7.08 (m, 2H), 6.73-6.71 (m, 4H), 6.64-6.58 (td, 1H), 6.46-6.40 (m, 1H), 6.00-5.97 (dd, 1H), 4.50 (s, 1H), 4.10-4.09 (d, 1H), 3.65-3.64 (d, 7H), 3.33-3.29 (dd, 1H), 2.55-2.49 (ddd, 1H), 2.41-2.34 (m, 1H), 2.20 (s, 1H), 1.65 (s, 4H). ¹³C NMR (100 MHz, CDCl₃): δ (ppm) 160.0, 158.7, 149.8, 149.4, 149.3, 144.6, 135.9, 135.7, 135.6, 130.2, 128.3, 128.0, 127.1, 113.3, 113.3, 106.7, 106.5, 106.2, 105.9, 105.9, 87.0, 86.5, 85.7, 72.1, 63.3, 55.3, 41.6.

5-Fluorobenzofuran modified 2'-deoxyuridine phosphoramidite substrate (4): To a solution of (3) (0.25 g, 0.38 mmol, 1 equiv) in anhydrous dichloromethane (5 mL) was added DIPEA (0.16 mL, 0.94 mmol, 2.5 equiv) and stirred for 10 min. All of these were added in N₂ environment. To this solution 2cyanoethyl N,N-diisopropylchlorophosphoramidite (0.101 mL, 0.451 mmol, 1.2 equiv) was added and the mixture was stirred for about 2.5 h. Then to the product ethyl acetate (50 mL) was added. The organic layer was washed with 5% sodium bicarbonate solution (20 mL) and brine solution (20 mL) successively, dried over sodium sulphate and evaporated to dryness. Column was done in 30% EtOAc in hexane. Obtained yield was 0.25 g. Percent yield is 67%.; ¹H NMR (CDCl₃, 400 MHz); δ (ppm) = 8.59 (s, 1H), 7.52-7.50 (d, 2H), 7.40-7.36 (dd, 5H), 7.26 (s, 1H), 7.22-7.18 (t, 2H), 7.12-7.06 (m, 2H), 6.72-6.70 (dd, 4H), 6.58-6.53 (td, 1H), 6.44-6.36 (m, 1H), 5.83-5.75 (ddd, 1H), 4.94-4.92 (dd, 1H), 4.61-4.55 (ddd, 1H), 4.23-4.18 (dd, 1H), 3.82-3.78 (dd, 1H), 3.71-3.68 (m, 2H), 3.65-3.64 (d, 6H), 3.60-3.45 (m, 4H), 3.26-3.22 (dd, 1H), 2.64-2.52 (m, 2H), 1.17-1.14 (dd, 12H).; ³¹P NMR: δ = 149.7.; .; HRMS: m/z Calculated for C₄₇H₅₁FN₄O₉P [M+H]⁺ = 865.3407, [M+Na]⁺ = 887.3208 found = 865.3379.

Synthesis of 5-Fluorobenzofuran-modified-2'-deoxyuridine (5): 100 mg (0.28 mmole, 1 equiv) of 2-deoxy-5-iodouridine, 0.179 g (0.423 mmole, 1.5 equiv) of stannylated FBF (fluorobenzofuran) and finally 3 mL of dioxane was added in N₂ conditions. Reaction mixture was degassed for about 40 min. Catalyst Pd(PPh₃)₂Cl₂ [Bis(triphenylphosphine) palladium (II) chloride] 9.89 mg (0.01 mmole, 0.05 equiv) was added and reaction mix was kept for heating in the oil bath at around 110°C. Reaction was kept for 3.5 hrs (approx.). TLC medium: 5% methanol, 0.2% TEA in DCM. Column was done in methanol, DCM system. Obtained yield is 0.052 g. yield percentage is 51%.; ¹H NMR (CDCl₃, 400MHz);δ (ppm) = 11.78 (s, 1H), 8.80 (s, 1H), 7.57-7.54 (dd, 1H), 7.45-7.43 (dd, 1H), 7.33 (s, 1H), 7.14-7.09 (td, 1H), 6.24-6.20 (t, 1H), 5.32-5.30 (t, 1H), 5.27-5.25 (t, 1H), 4.35-4.31 (m, 1H), 3.88 (d, 1H), 3.75-3.64 (m, 3H).

Synthesis of 5-Fluorobenzofuran-modified uridine (7):100 mg (0.27 mmole, 1 equiv) of 2-deoxy-5-iodouridine, 0.17 g (0.41 mmole, 1.5 equiv) of stannylated FBF (fluorobenzofuran) and finally 3 mL of dioxane was added in N₂ conditions. Reaction mixture was degassed for about 40 min. Catalyst Pd(PPh₃)₂Cl₂

[Bis(triphenylphosphine) palladium (II) chloride] 9.47 mg (0.01 mmole, 0.1 equiv) was added and reaction mix was kept for heating in the oil bath at around 110°C. Reaction was kept for 3.5 hrs. TLC medium: 5% methanol, 0.2% TEA in DCM. Column was done in methanol, DCM system. Obtained yield was 56.2 mg. Yield percentage is 55%.; ¹H NMR (CDCl₃, 400MHz); δ (ppm) = 11.8 (s, 1H), 8.93 (s, 1H), 7.58-7.54 (dd, 1H), 7.45-7.42 (dd, 1H), 7.33 (s, 1H), 7.14-7.19 (td, 1H), 5.86-5.85 (d, 1H), 5.50-5.49 (d, 1H), 5.41-5.39 (t, 1H), 5.13-5.12 (d, 1H), 4.15-4.07 (dt, 2H), 3.96 (s, 1H), 3.82-3.79 (d, 1H), 3.69-3.66 (d, 1H).

Solid phase DNA synthesis of H-telo (10) and bcl2 (8): fluorobenzofuran modified H-telo (10) and bcl2 (8) were synthesized (1 μmole scale, 1000 Å CPG solid support) by standard oligonucleotide synthesis protocol of phosphoramidite. The solid support after final detritylation step was treated with 30% aqueous ammonium hydroxide solution. Solution was then evaporated using speed vac and finally residue was purified by denaturing PAGE (20% gel). The band corresponding to modified sequences was identified by performing UV shadowing, it was then cut and transferred to a Poly-Prep column. The gel pieces were crushed using a sterile glass rod, and modified sequences was extracted using ammonium acetate buffer (0.5 M, 3 mL) for 12 h and desalted using Sep-Pak column. The purity of modified sequences was confirmed by reverse phase HPLC and characterized by LCMS.; m/z theoretical of 10 and 8 :7250.81 g and 11675.51 g respectively; m/z experimental of 10 and 8: 7250.38 g and 11675.25 g.

Steady state fluorescence: For steady-state fluorescence study, nucleoside 7 (1 μM) was excited at 322 nm in a micro fluorescence cuvette (Hellma, path length 10 mm) on Fluoromax-4 spectrofluorometer. Fluorescence experiments were performed in duplicates. Modified ONs 10 (H-telo) and 8 (bcl2) (0.5 μM) were heated for 3 min at 93 °C in sodium phosphate buffer or in acetate buffer (30 mM, pH range 5.0 – 7.9) containing 50 mM NaCl and then samples were allowed to come to room temperature over a period of 2 - 3 h. ONs samples were excited at 330 nm in micro fluorescence cuvette (Hellma, path length 10 mm) on Fluoromax-4 spectrofluorometer with an excitation and emission slit width 3 mm and 3 mm,

respectively. All fluorescence experiments with nucleoside and oligonucleotides were performed in duplicates.

Dynamic Light Scattering (DLS): Nucleoside **7** (1 μM) was added to solution containing AOT of different concentration such that the samples would have appropriate W_o value. Concentration of **7** was kept fixed and concentration of AOT was adjusted accordingly. Afterwards samples were kept in dark for 3 h (incubation time for RM). Analysis was performed to determine the size of the particle. DLS analysis was done in duplicates.

Steady-state fluorescence of 6 inside AOT reverse micelles with different W_o values: Nucleoside **7** (1 μM) was added to solution containing AOT of different concentration such that the samples would have appropriate W_o value. Concentration of **7** was kept fixed and concentration of AOT was adjusted accordingly. Afterwards, samples were kept in dark for 3 h. For steady-state fluorescence study, **7** (1 μM) was excited at 322 nm. Fluorescence experiments were performed in triplicate in micro fluorescence cuvette (Hellma, path length 10 mm) on Fluoromax-4 spectrofluorometer. Anisotropy measurements were performed in triplicate and each anisotropy value was an average of 10 successive measurements. For steady-state lifetime study, samples of different W_o were excited at its respective λ emission. λ emission of samples having different W_o were determined in fluorescence. Lifetime experiments were performed in triplicate in micro fluorescence cuvette (Hellma, path length 10 mm).

Fluorescence of modified ON 10 (H-telo) in RM: Modified ON **10** (0.5 μM) was heated for 3 min at 93 $^{\circ}\text{C}$ in sodium phosphate buffer or in acetate buffer (30 mM, pH range 5.0 – 7.9) containing 50 mM NaCl and then samples were allowed to come to room temperature over a period of 2 - 3 h. Sample containing ON **10** was injected in appropriate amount of AOT such that the size of reverse micelles is W_o 20. Sonication was done for 30 seconds and samples were kept in dark for 3 h. Samples were excited at 330 nm in micro fluorescence cuvette (Hellma, path length 10 mm) on Fluoromax-4 spectrofluorometer with an excitation and emission slit width 3 mm and 3 mm, respectively. Fluorescence spectra were recorded in duplicates.

Circular dichorism of modified ONs 10, 8 and control unmodified 11, 9 (CD): ONs 10, 8 and 11, 9 (5 μM) were heated for 3 min at 93 °C in sodium phosphate acetate buffer (30 mM, pH range 5.0 – 7.9) containing 50 mM NaCl and after that samples were allowed to come to room temperature over a period of 2 – 3 h. CD spectra were recorded in a quartz cuvette (Starna Scientific, path length 5 mm) on a J-815 CD spectropolarimeter (Jasco, USA) using 1 nm bandwidth at 25°C from 210 to 320 nm. Each CD profile obtained was an average of five scans collected at a scan speed of 100 nm min⁻¹. CD measurements were performed in duplicate. All spectra were corrected using an appropriate blank solution in the absence of sequence.

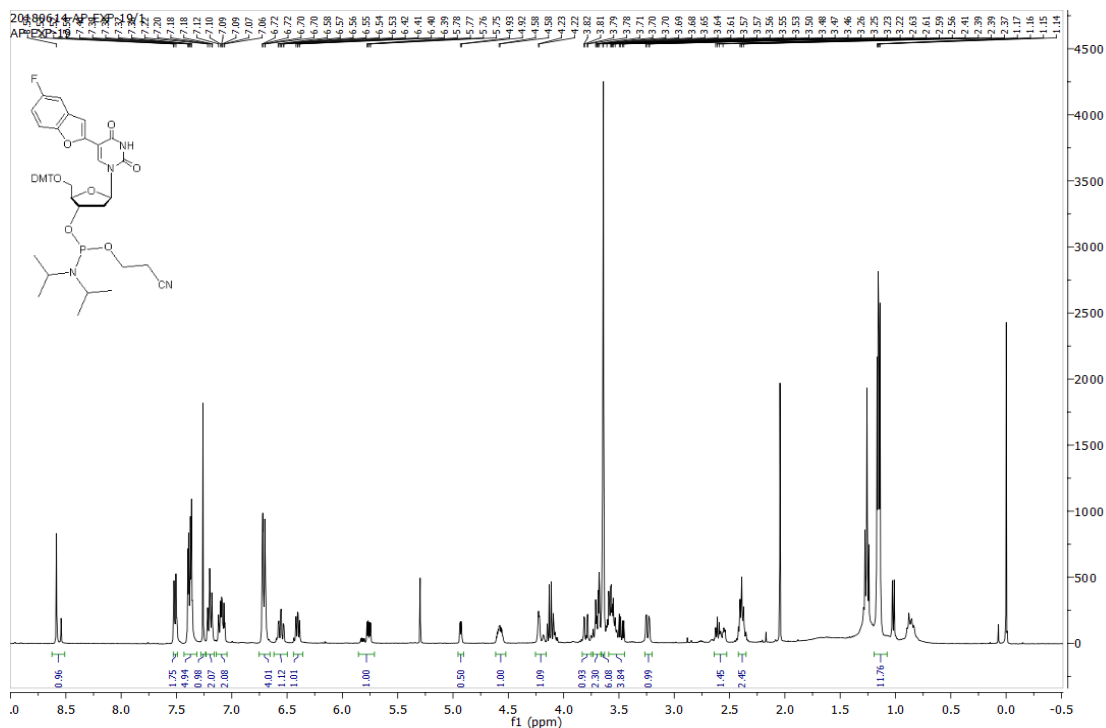
Thermal Melting analysis of ONs 10 and 8 (T_m): Modified ONs 10 and 8 (1 μM) were heated for 3 min at 93 °C in sodium phosphate or acetate buffer (30 mM, pH range 5.0 – 7.9). Samples were allowed to come to room temperature over a period of 2 – 3 h. T_m was performed using instrument Cary 300 Bio UV-Vis spectrophotometer. The temperature was subsequently increased from 20 °C to 90 °C at 1 °C min⁻¹. Absorbance was measured at 295 nm in every 1 °C interval.

Circular dichorism of modified ONs 10 , 8 and control unmodified ONs 11, 9 in RM: ONs 10 (H-telo), 8 (bcl-2) and 11, 9 (5 μM) were heated for 3 min at 93 °C in sodium phosphate or acetate buffer (30 mM, pH range 5.0 – 7.4) containing 50 mM NaCl and then samples were allowed to come to room temperature over a period of 2 – 3 h. Samples containing ONs was injected in appropriate amount of AOT such that the size of reverse micelles is W_o 20. Sonication was done for 30 seconds and samples were kept in dark for 3 h. CD spectra was recorded in a quartz cuvette (Starna Scientific, path length 5 mm) on a J-815 CD spectropolarimeter (Jasco, USA) using 1 nm bandwidth at 25°C from 210 to 320 nm. Each CD profile obtained was an average of five scans collected at a scan speed of 100 nm min⁻¹. CD measurements were performed in duplicate. All spectra were corrected using an appropriate blank solution in the absence of sequence.

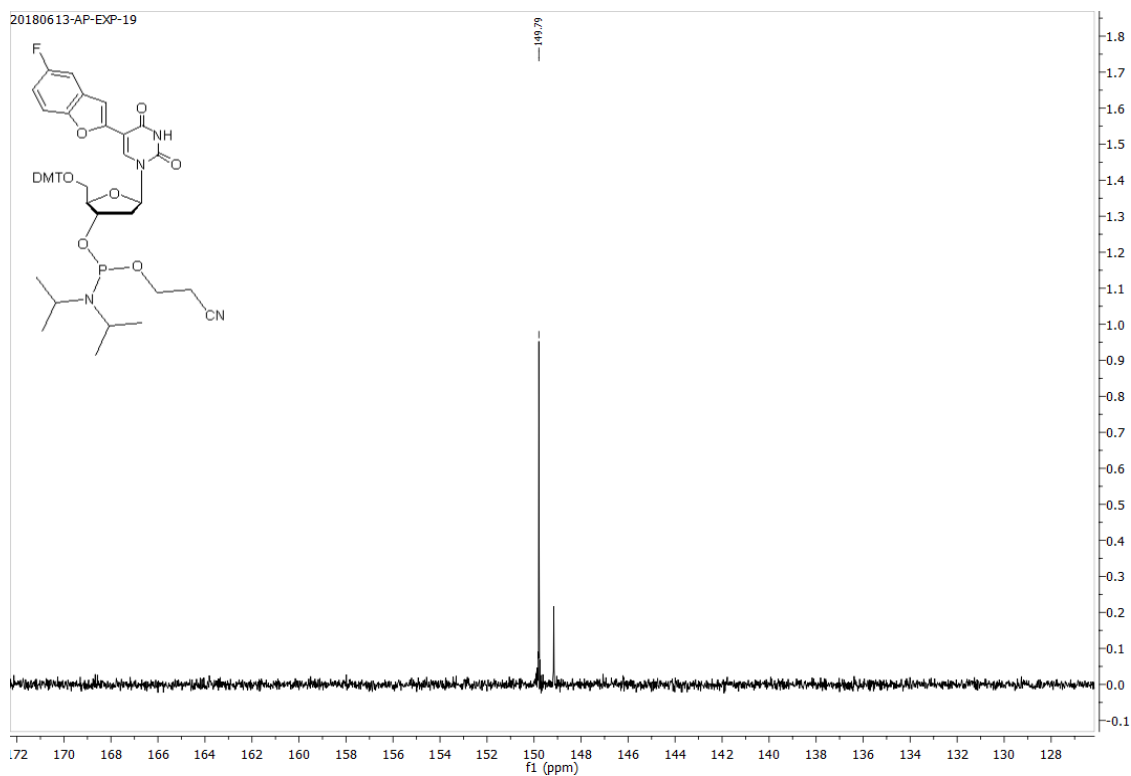
Sample preparation for ^{19}F and ^1H NMR analysis of H-telo DNA (10) and bcl2 DNA (8) ONs: Phosphate and acetate buffer; H-telo DNA ONs (100 μM) and bcl2 DNA ONs (200 μM) were annealed in acetate or phosphate buffer by heating samples for 3 min at 93 $^{\circ}\text{C}$ into i-motifs. Samples were then allowed to cool down to room temperature and then were transferred into Shigemi tube (5 mm advance NMR microtube) for NMR analysis.

Appendix /Supporting information

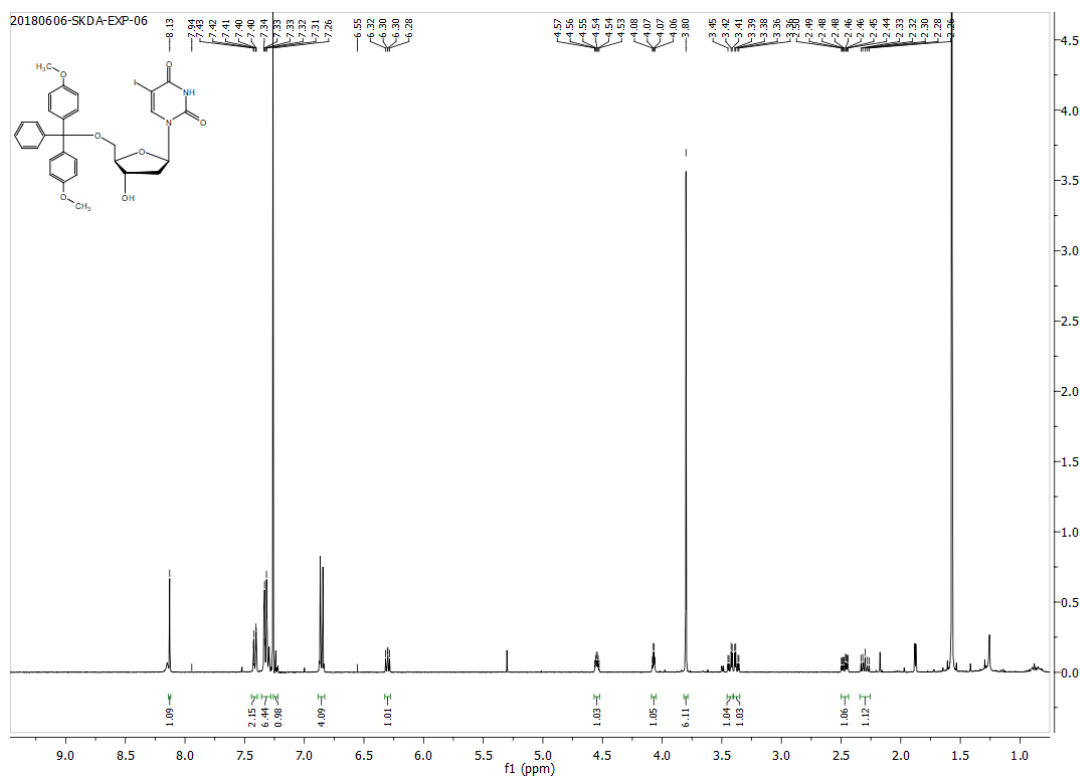
¹H NMR 5-Fluorobenzofuran modified 2'-deoxyuridine phosphoramidite substrate (4)



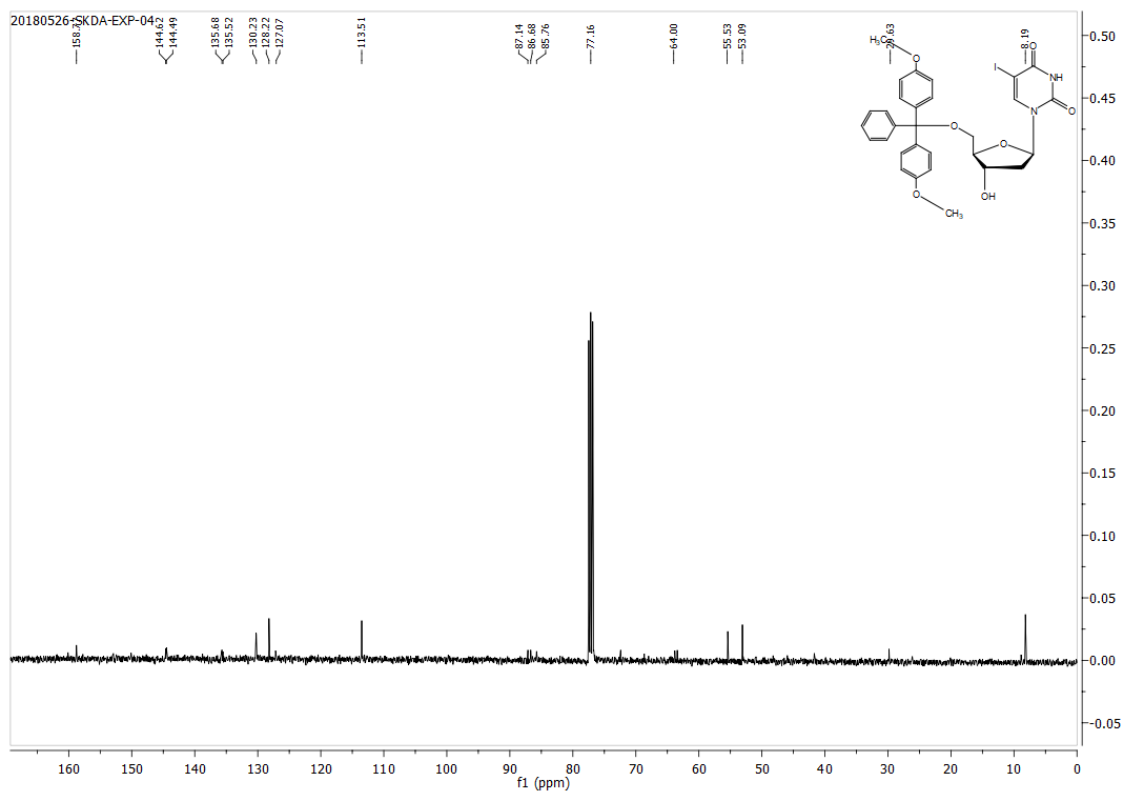
³¹P NMR 5-Fluorobenzofuran modified 2'-deoxyuridine phosphoramidite substrate (4)



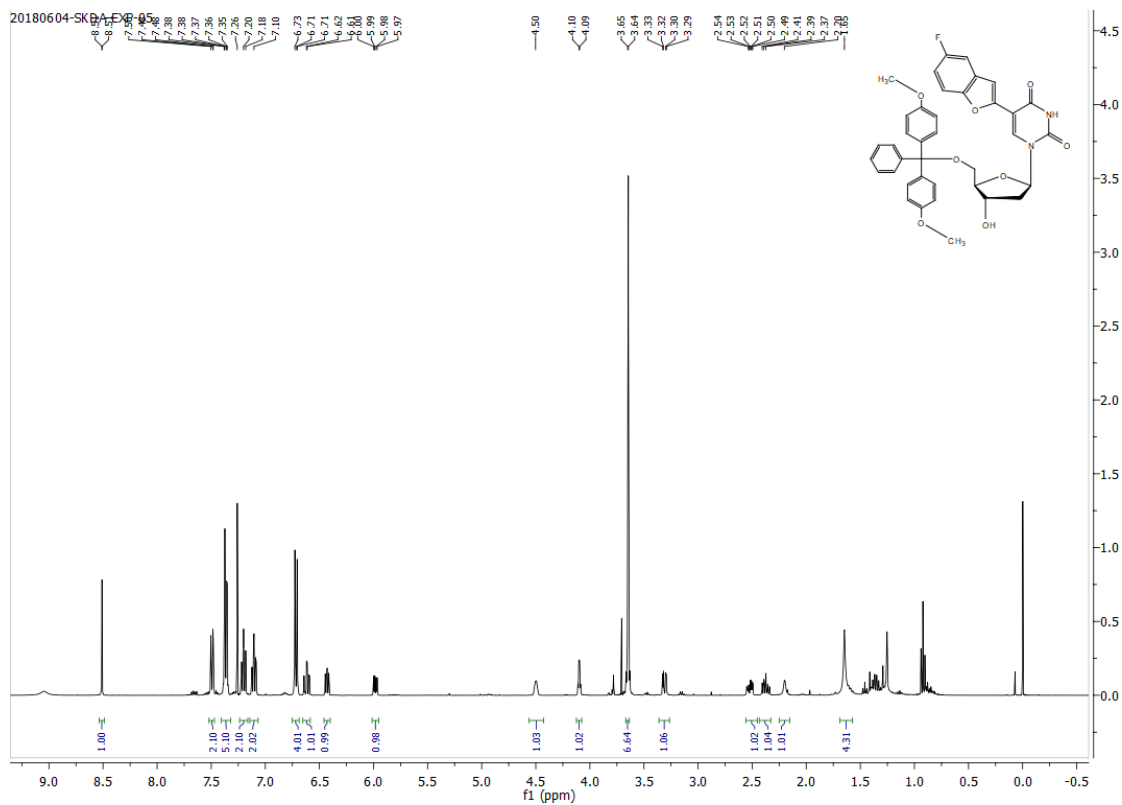
¹H NMR DMT protected 5-iodo-2'-deoxyuridine (2)



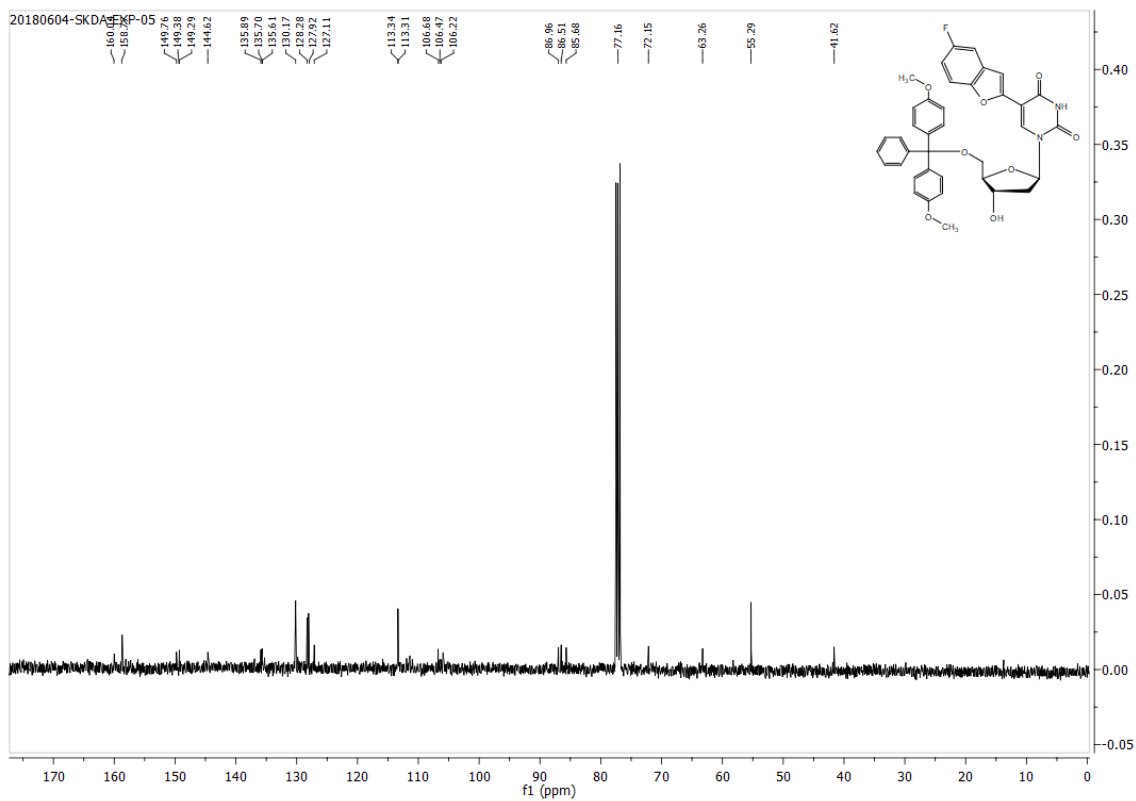
¹³C NMR of DMT protected 5-iodo-2'-deoxyuridine (2)



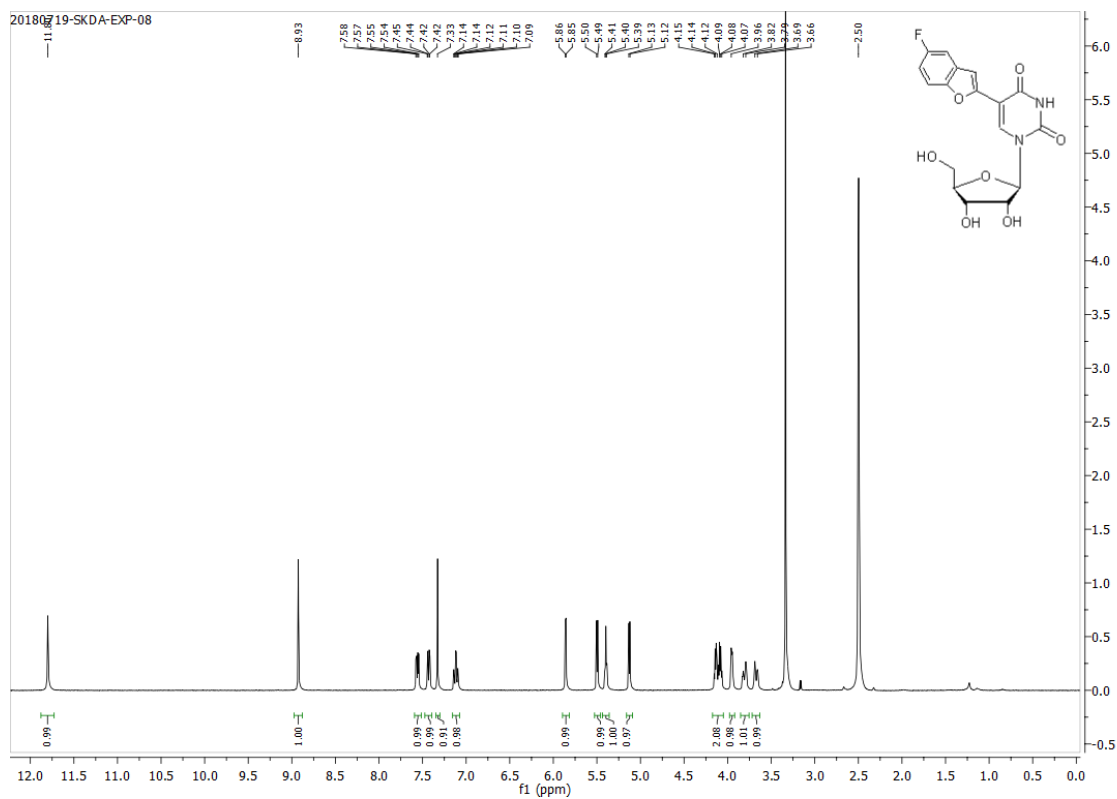
¹H NMR 5-Fluorobenzofuran-modified 5'-O-DMT-2'-deoxyuridine (3)



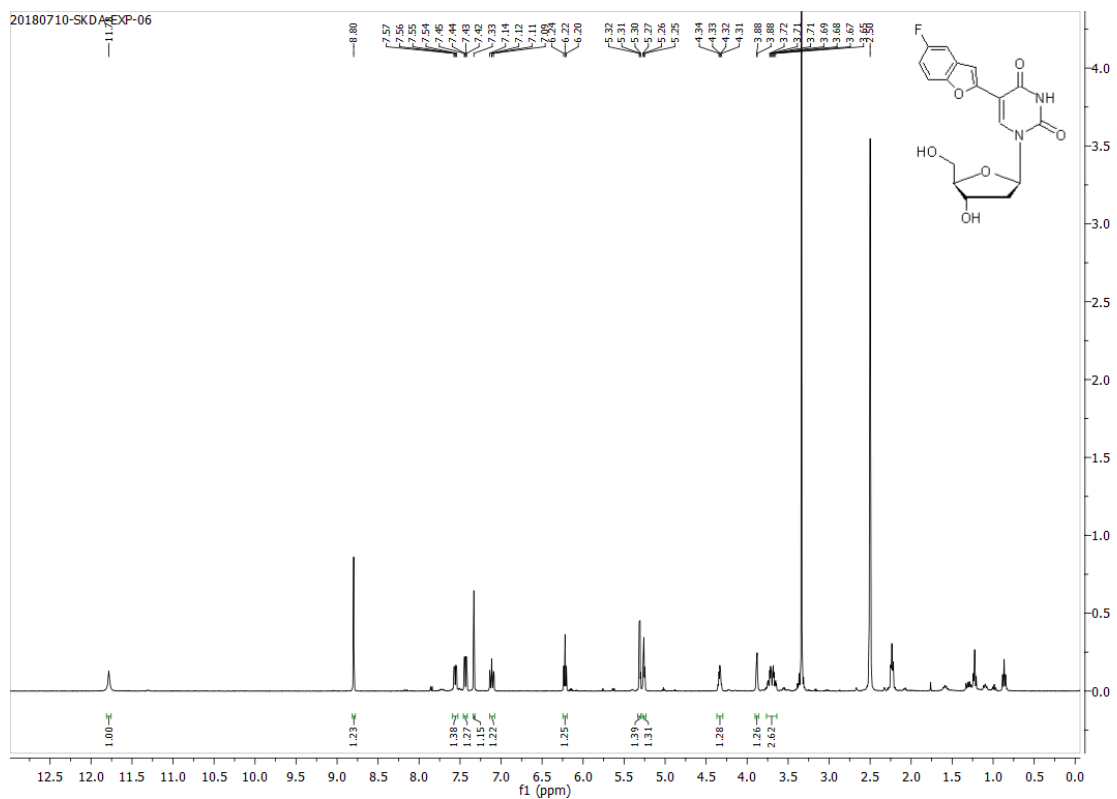
¹³C NMR of 5-Fluorobenzofuran-modified 5'-O-DMT-2'-deoxyuridine (3)



¹H NMR of 5-Fluorobenzofuran-modified uridine (7)



¹H NMR of 5-Fluorobenzofuran-modified-2'-deoxyuridine (5)

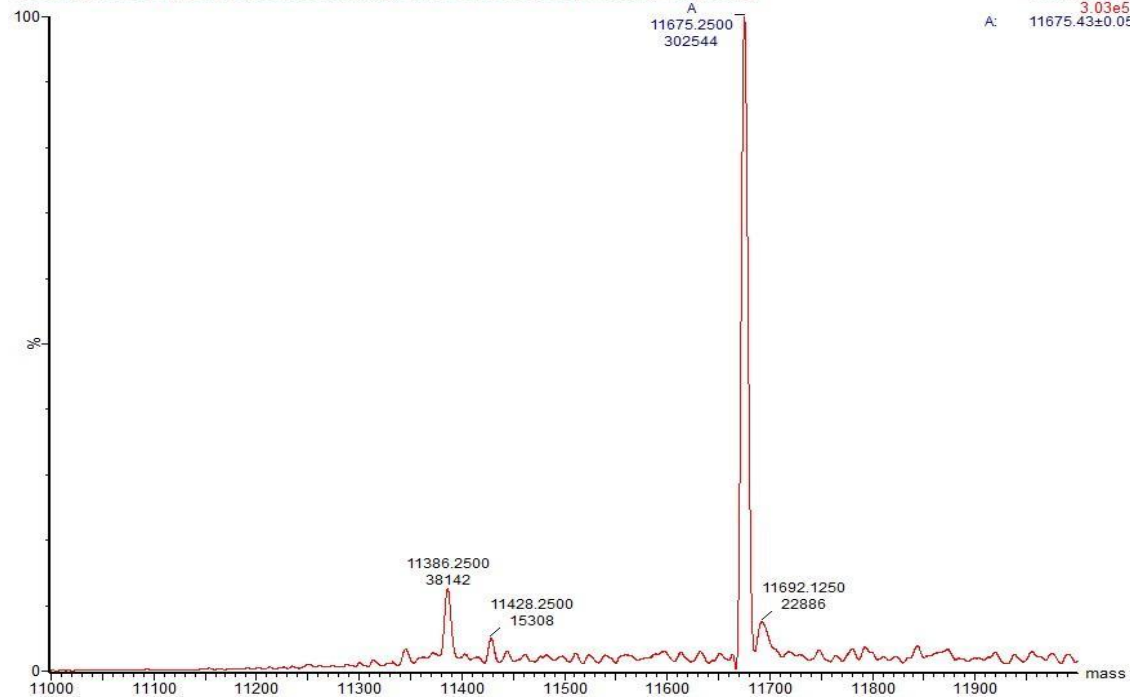


bcl2 (b cell lymphoma) (8)

port A, 50L/min, sample needle, 100pmol

10092018_BCL2 59 (1.024) Tr (600:2000,0.13,Mid); Sm (SG, 5x20.00); Sb (25,10.00); Cm (10:110)

TOF MS ES-
3.03e5
A: 11675.43±0.05

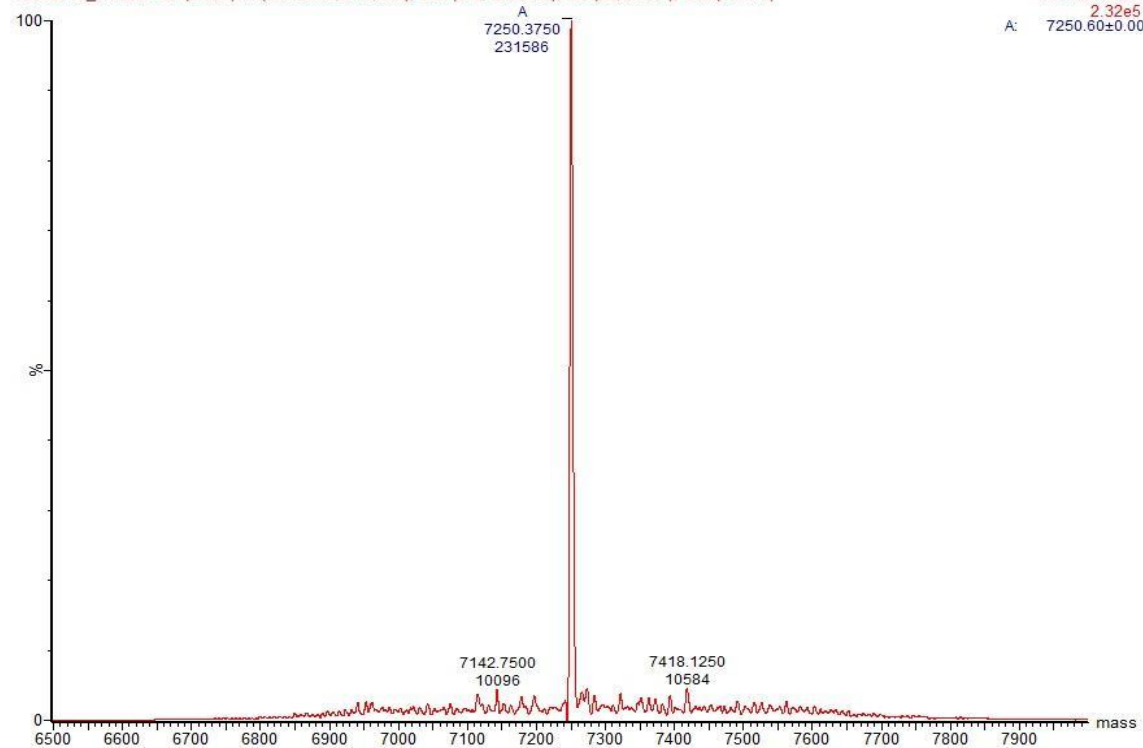


H – telo (Human Telomerase) (10)

port A, 50L/min, sample needle, 100pmol

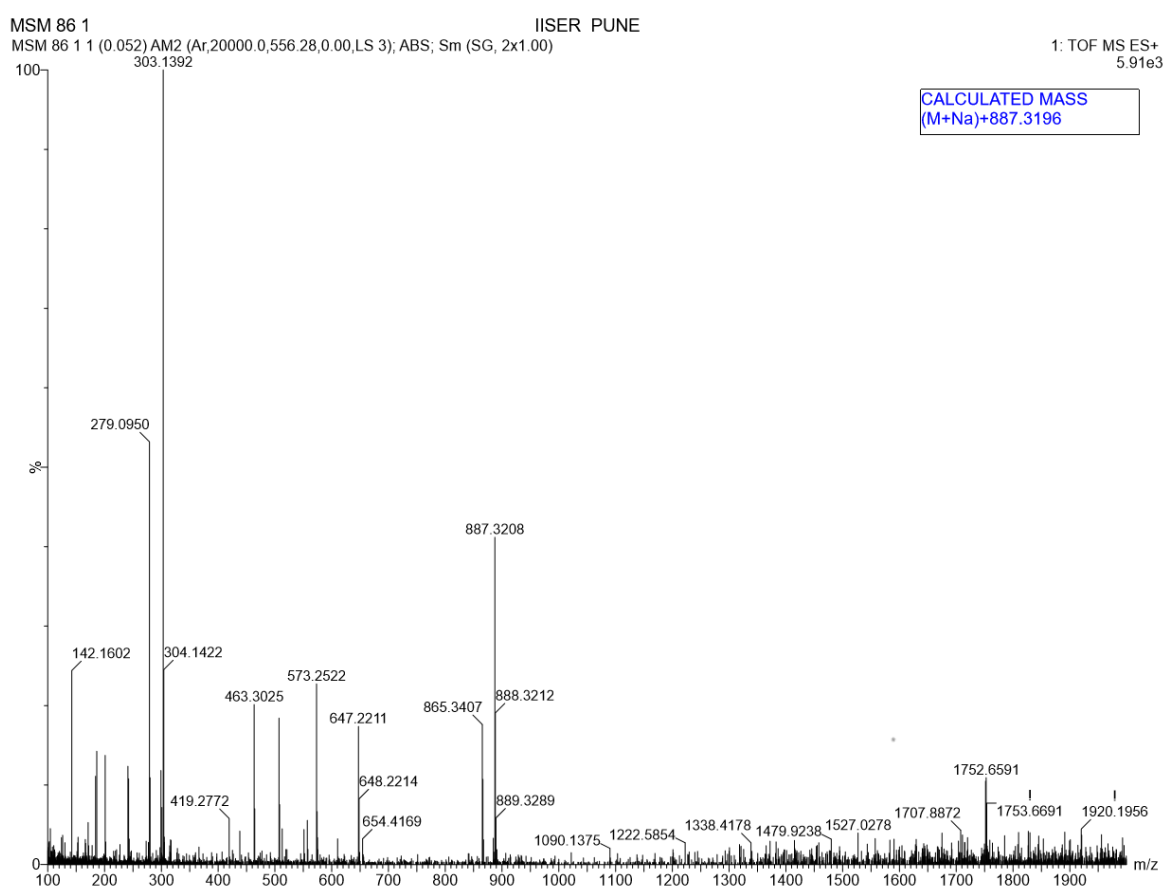
10092018_HTELO 28 (0.495) Tr (600:2000,0.13,Mid); Sm (SG, 5x20.00); Sb (25,10.00); Cm (10:110)

TOF MS ES-
2.32e5
A: 7250.60±0.00

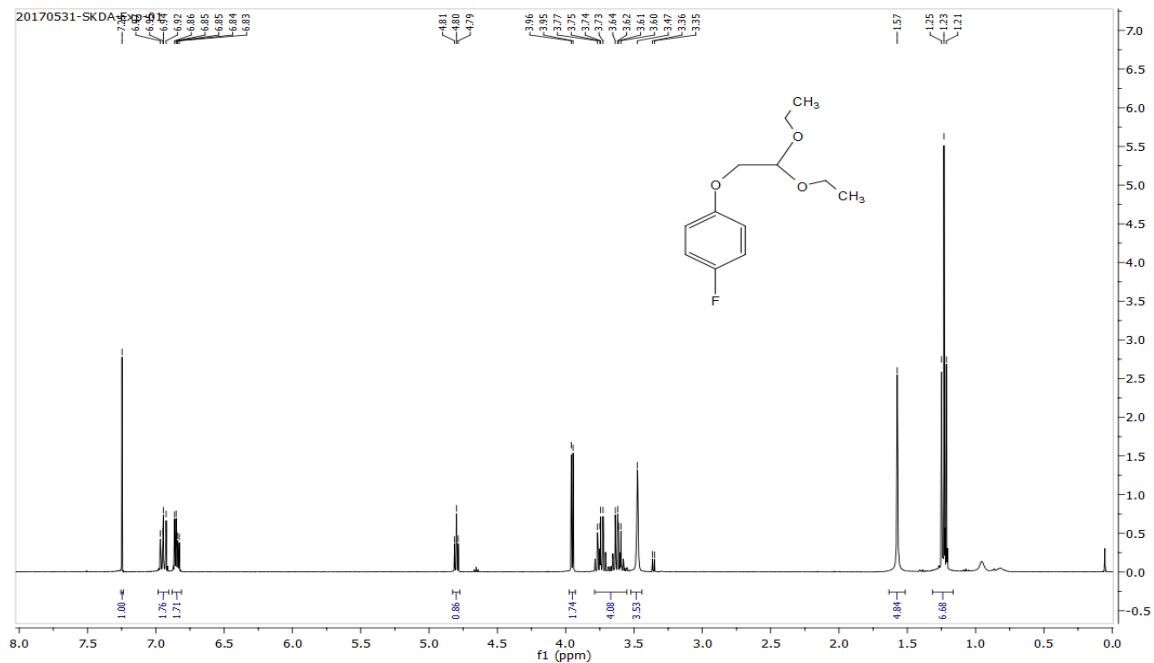


Sequence name	Theoretical mass (g)	Experimental mass (g)
H-Telo (10)	7250.81	7250.38
bcl2 (8)	11675.51	11675.25

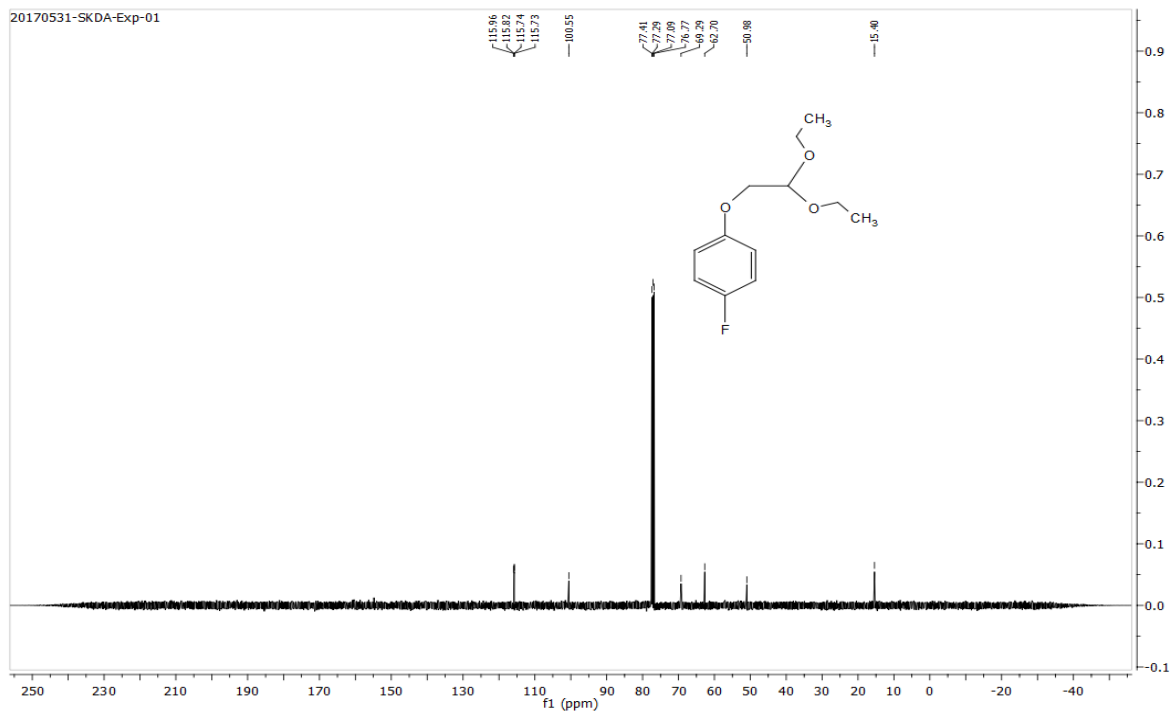
HRMS of 5-Fluobenzofuran modified 2'-deoxyuridine phosphoramidite



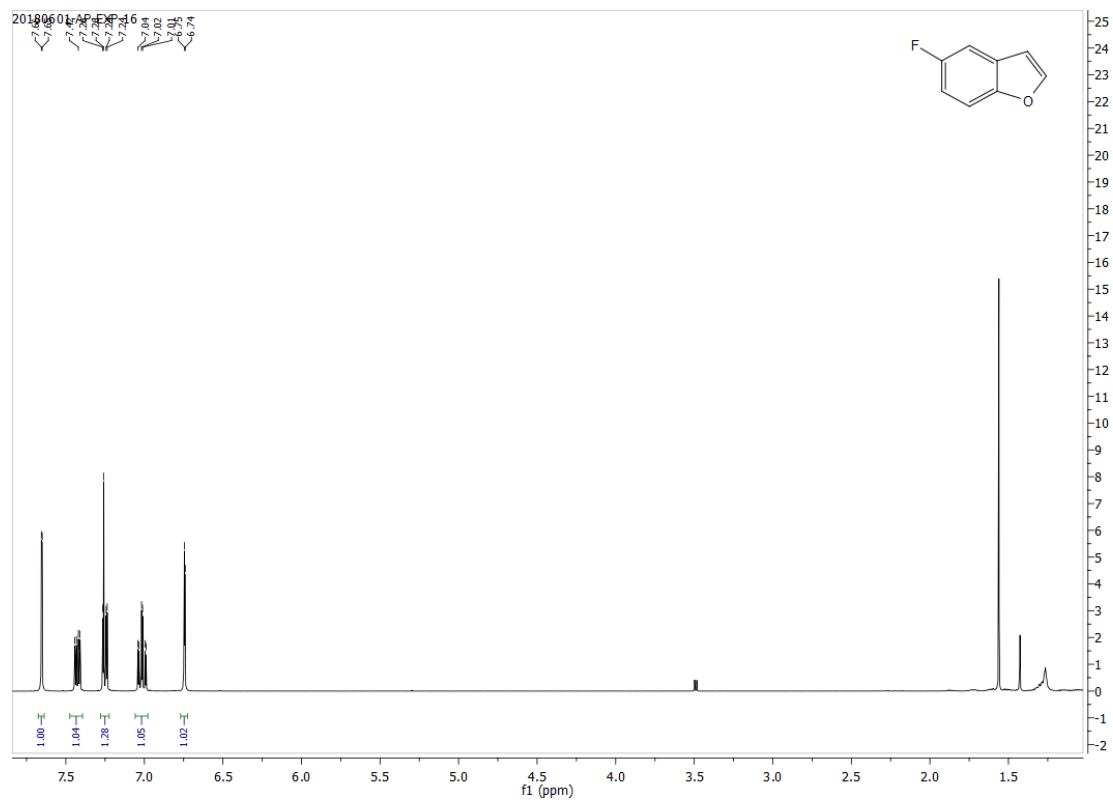
¹H NMR of 4-Fluorophenoether 1(c)



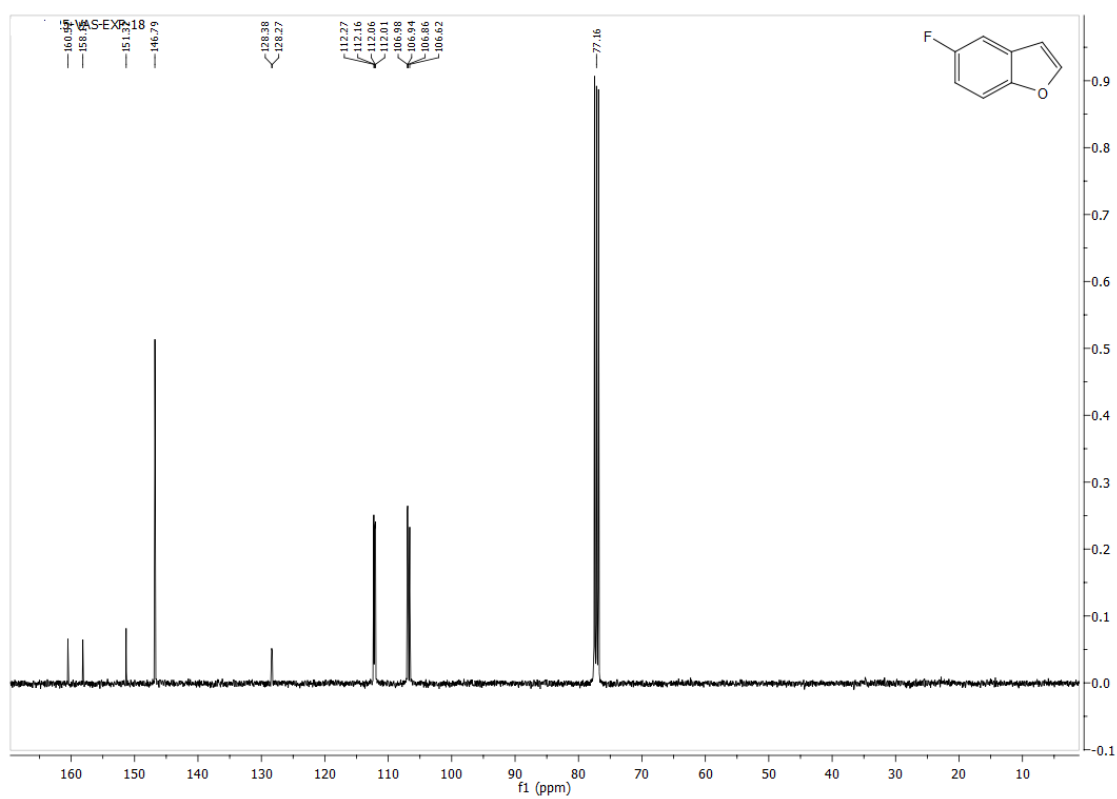
¹³C NMR of 4-Fluorophenoether 1(c)



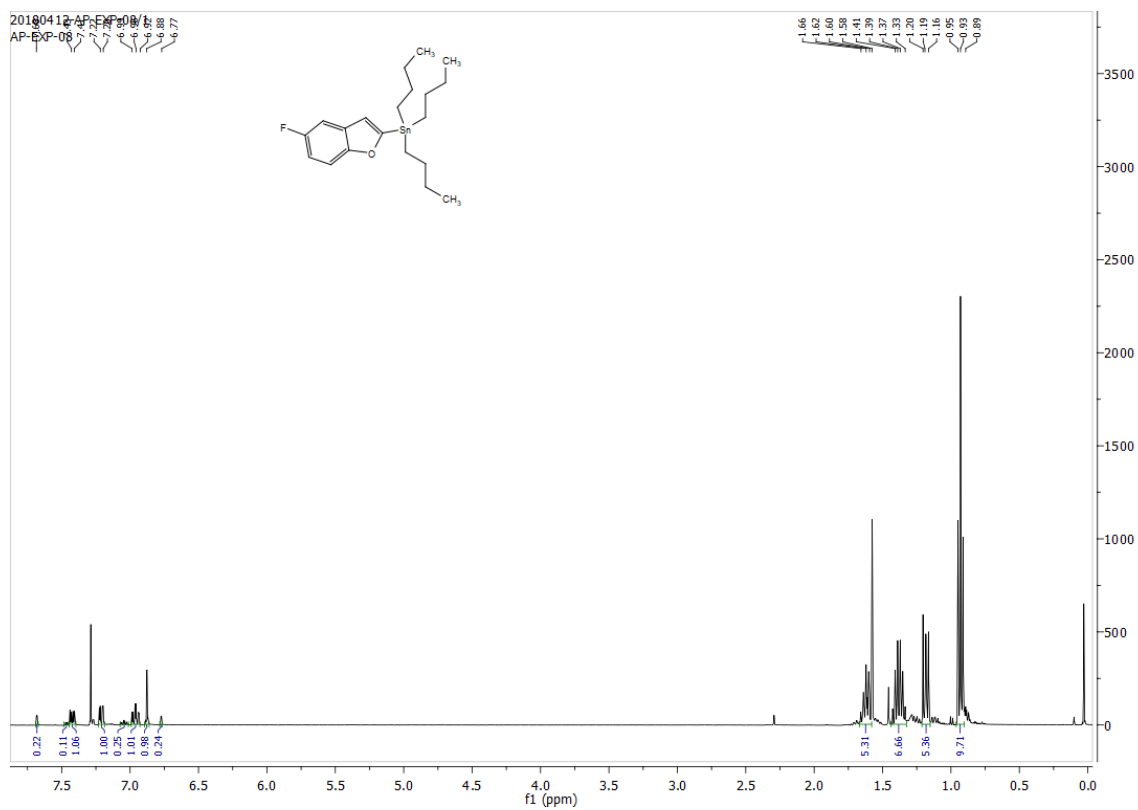
¹H NMR of 5-fluorobenzofuran **1(d)**



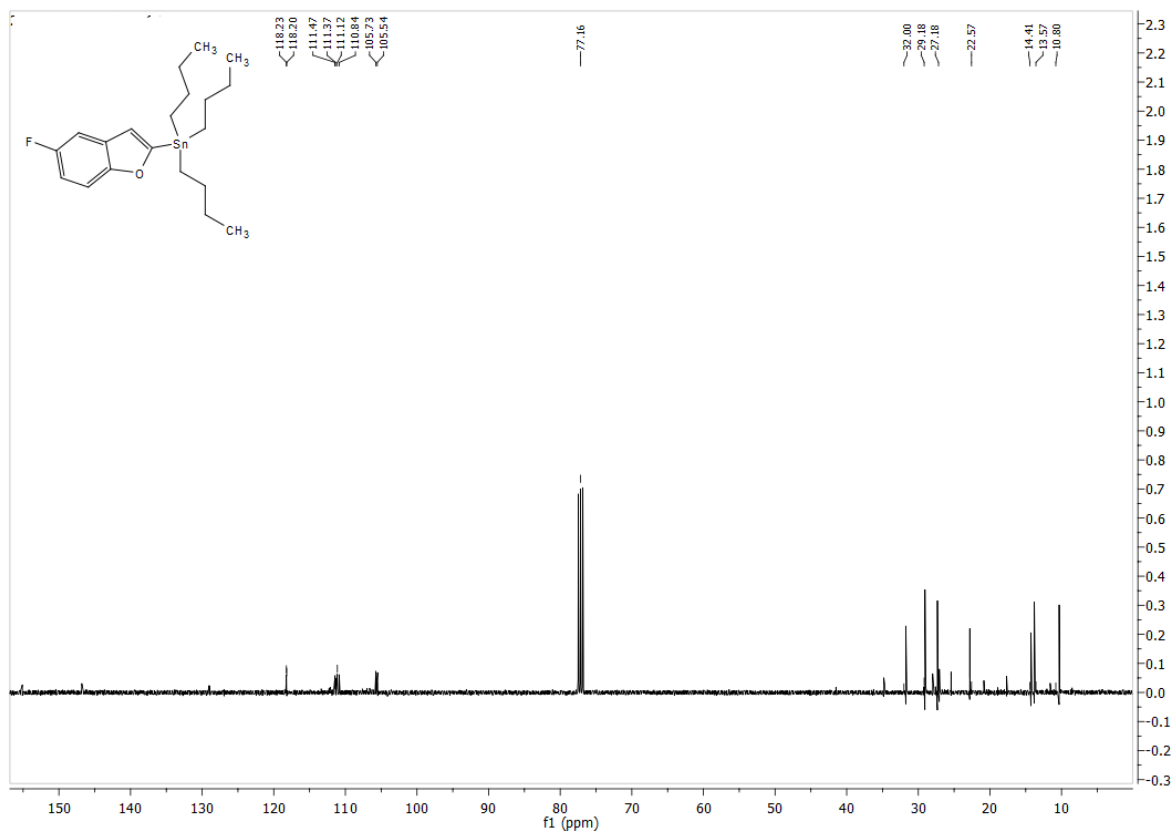
¹³C NMR of 5-fluorobenzofuran **1(d)**



¹H NMR of stannylated fluorobenzofuran **1(e)**



¹³C NMR of stannylated fluorobenzofuran **1(e)**



References:

1. Arun A. Tanpure.; Maroti G. Pawar.; Seergazhi G. Srivatsan.; Fluorescent Nucleoside Analogs: Probes for Investigating Nucleic Acid Structure and Function. *Isr. J. Chem.* **2013**, *53*, 366–378.
2. G. W. Collie.; G. N. Parkinson.; The application of DNA and RNA G-quadruplexes to therapeutic medicines.; *Chem. Soc. Rev.*, **2011**, *40*, 5867–5892.
3. T. A. Brooks.; S. Kendrick.; L. Hurley.; Making sense of G-quadruplex and i-motif functions in oncogene promoters.; *FEBS J.*, **2010**, *277*, 3459–3469.
4. Jussara Amato.; Nunzia Iaccarino.; Antonio Randazzo.; Ettore Novellino.; Bruno Pagano.; Noncanonical DNA Secondary Structures as Drug Targets: the Prospect of the i-Motif. *ChemMedChem*, **2014**, *9*, 2026-2030.
5. S. Balasubramanian.; L. H. Hurley.; S. Neidle.; Targeting G-quadruplexes in gene promoters: a novel anticancer strategy? *Nat. Rev. Drug Discovery*, **2011**, *10*, 261–275.
6. Pramod M. Sabale.; Arun A. Tanpure.; Seergazhi G. Srivatsan.; Probing the competition between duplex and G-quadruplex/i-motif structures using a conformation-sensitive fluorescent nucleoside probe. *Org.Biomol.Chem*, **2018**, *16*, 4141- 4150.
7. Sudeshna Manna.; Cornelia H. Panse.; Vyankat A. Sontakke.; Sarangamath Sangamesh.; Seergazhi G. Srivatsan.; Probing Human Telomeric DNA and RNA Topology and Ligand Binding in a Cellular Model by Using Responsive Fluorescent Nucleoside Probes.; *ChemBioChem*, **2017**, *18*,1604–1615.
8. Arun A. Tanpure.; Seergazhi G. Srivatsan.; Conformation-sensitive nucleoside analogues as topology-specific fluorescence turn-on probes for DNA and RNA G-quadruplexes.; *Nucleic Acids Res.* **2015**, *43*, e149.
9. Henry A, Pavlos P, Zoe A.E Waller; i-motif DNA: Structure, stability and targeting with ligands. *Bioorg. Med. Chem.* **2014**, *22*, 4407–4418.
10. D. Sun.; L. H. Hurley.; The Importance of Negative Superhelicity in Inducing the Formation of G-Quadruplex and i-Motif Structures in the c-Myc Promoter: Implications for Drug Targeting and Control of Gene Expression.; *J. Med. Chem.*, **2009**, *52*, 2863–2874.

11. A. Rajendran.; S. Nakano.; N. Sugimoto.; Molecular crowding of the cosolutes induces an intramolecular i-motif structure of triplet repeat DNA oligomers at neutral pH.; *Chem. Commun.*, **2010**, *46*, 1299–1301.
12. J. A. Brazier, A. Shah and G. D. Brown, I-Motif formation in gene promoters: unusually stable formation in sequences complementary to known G-quadruplexes.; *Chem. Commun.*, **2012**, *48*, 10739–10741.
13. Henry A. Day.; Camille Huguin.; Zoë A. E. Waller.; Silver cations fold i-motif at neutral pH.; *Chem. Commun.*, **2013**, *49*, 7696–7698.
14. Zeraati, M., Langley, D. B., Schofield, P., Moye, A. L., Rouet, R., Hughes, W. E., Bryan, T. M., Dinger, M. E. and Christ, D. (2018) I-motif DNA structures are formed in the nuclei of human cells. *Nat Chem*, **2018**, *10*, 631–637.
15. Hala Abou Assi.; Miguel Garavís.; Carlos González.; Masad J Damha; i-Motif DNA: structural features and significance to cell biology, *Nucleic Acids Research*, **2018**, *46*, 8038–8056.
16. Souvik Modi.; Swetha M. G.; Debanjan Goswami.; Gagan D. Gupta.; Satyajit Mayor and Yamuna Krishnan: A DNA nanomachine that maps spatial and temporal pH changes inside living cells. *Nat. Nanotechnol.* **2009**, *4*, 325–340.
17. A. M. Fleming.; Y. Ding, R. A. Rogers.; J. Zhu, J. Zhu.; A. D. Burton.; C. B. Carlisle.; C. J. Burrows.; $4n-1$ Is a “Sweet Spot” in DNA i-Motif Folding of 2'-Deoxycytidine Homopolymers. *J. Am. Chem. Soc.*, **2017**, *139*, 4682–4689.
18. J. Lee II.; B. H. Kim. Monitoring i-motif transitions through the exciplex emission of a fluorescent probe incorporating two ^{Py}A units. *Chem. Commun.*, **2012**, *48*, 2074–2076.
19. G. Mata .; N. W. Luedtke.; Fluorescent Probe for Proton-Coupled DNA Folding Revealing Slow Exchange of i-Motif and Duplex Structures. *J. Am. Chem. Soc.*, **2015**, *137*, 699–707.
20. P. S.-W. Yeung.; P. H. Axelsen.; The Crowded Environment of a Reverse Micelle Induces the Formation of β -Strand Seed Structures for Nucleating Amyloid Fibril Formation. *J. Am. Chem. Soc.* **2012**, *134*, 6061–6063.
21. Maroti G. Pawar, and Seergazhi G. Srivatsan.; An Environment-Responsive Fluorescent Nucleoside Analog Probe for Studying Oligonucleotide Dynamics in a Model Cell-Like Compartment. *J. Phys. Chem. B*, **2013**, *117*, 14273–14282.

22. Manna, S.; Srivatsan, S. G.; Fluorescence-based tools to probe G-quadruplexes in cell-free and cellular environments. *RSC Adv.*, **2018**, *8*, 25673-25694.
23. Mahdi Zeraati, David B. Langley¹, Peter Schofield¹, Aaron L. Moye, Romain Rouet, William E. Hughes, Tracy M. Bryan, Marcel E. Dinger and Daniel Christ.; I-motif DNA structures are formed in the nuclei of human cells. *Nature Chemistry*, **2018**, *10*, 631–637.
24. Debbie C. Crans And Nancy E. Levinger.; The Conundrum of pH in Water Nanodroplets: Sensing pH in Reverse Micelle Water Pools.; *Accounts Of Chemical Research*, **2012**, *10*, 1637-1645.
25. Sudeshna Manna.; Debayan Sarkar.; and Seergazhi G. Srivatsan.; A Dual-App Nucleoside Probe Provides Structural Insights into the Human Telomeric Overhang in Live Cells.; *J. Am. Chem. Soc.*, **2018**, *140*, 39, 12622-12633.
26. Laurie Lannes.; Saheli Halder.; Yamuna Krishnan.; Harald Schwalbe.; Tuning the pH Response of i-Motif DNA Oligonucleotides.; *ChemBioChem*, **2015**, *16*, 1647–1656.
27. Guillaume Mata.; Nathan W. Luedtke.; Fluorescent Probe for Proton-Coupled DNA Folding Revealing Slow Exchange of i-Motif and Duplex Structures.; *J. Am. Chem. Soc.*, **2015**, *137*, 699–707.
28. K. Snoussi.; J.-L. Leroy.; Imino Proton Exchange and Base-Pair Kinetics in RNA Duplexes.; *Biochemistry*, **2001**, *40*, 8898-8904.